Review

Polyamidoamine dendrimer-based materials for environmental applications: A review

Herlys Viltres [a], Yeisy C. López [a,b], Carolina Leyva [a], Nishesh Kumar Gupta [c,d], Adrián Ges Naranjo [e], Próspero Acevedo–Peña [a], Alejandro Sanchez-Diaz [f], Jiyeol Bae [c,d], Kwang Soo Kim [c,d,∗]

[a] Instituto Politécnico Nacional, Centro de Investigación en Ciencia Aplicada y Tecnología Avanzada, CDMX, Mexico
[b] Universidad de La Habana, Facultad de Química, Laboratorio de Bioninorgánica, La Habana, Cuba
[c] University of Science and Technology (UST), Daejeon, Republic of Korea
[d] Department of Land, Water, and Environment Research, Korea Institute of Civil Engineering and Building Technology (KICT), Goyang, Republic of Korea
[e] Departamento de Radioquímica, Facultad de Ciencias y Tecnologías Nucleares, Instituto Superior de Tecnologías y Ciencias Aplicadas, La Habana, Cuba
[f] Universidad de Colima, Facultad de Ciencias Químicas, Laboratorio de Materiales, Colima, Mexico

ARTICLE INFO

ABSTRACT

The development of efficient adsorbents for environmental applications has been prioritized, considering the increasing pollution worldwide. The continuous search for new and effective materials has led to the development of polyamidoamine (PAMAM) dendrimer-based materials for their use in wastewater treatment, precious metal recovery, sensing, and CO_2 capture. PAMAM with a three-dimensional branched architecture, accessible internal cavities, and easy surface functionalization are suitable for removing inorganic (radionuclides, heavy metals, and precious metal ions) and organic (dyes, drugs, and pesticides) pollutants. Moreover, a large number of terminal amines of PAMAM dendrimer serve as a suitable platform for CO_2 capture and conversion. This review is intended to provide the readers with an updated overview of PAMAM-based adsorbents and their role in the removal and recovery of various inorganic and organic pollutants. PAMAM-based materials as a sensor for pollutants detection and quantification has been discussed. Also, environmental considerations related to the use of PAMAM-based materials have been included.

© 2021 Elsevier B.V. All rights reserved.

Contents

∗ Corresponding author at: University of Science and Technology (UST), Daejeon, Republic of Korea.
   E-mail address: kskim@kict.re.kr (K.S. Kim).

Abbreviations and nomenclatures

Alg/Hal_PAMAM beads encapsulation of polyamidoamine dendrimer functionalized halloysite nanotubes in alginate

Alg/Hal_PAMAM beads encapsulation of polyamidoamine-functionalized halloysite nanotubes in alginate

Amine-functionalized α-Fe$_2$O$_3$ nanofiber polyamidoamine grafted α-Fe$_2$O$_3$ nanofiber

CCMD carboxymethyl chitosan-modified magnetic-cored dendrimers

CS-G3 third generation of polyamidoamine-grafted chitosan

CT-HPMNPs carboxyl-terminated hyperbranched polyamidoamine dendrimers (Generation 5.5) grafted superparamagnetic nanoparticles

CTS chitosan functionalized polyamidoamine dendrimer

DF-MNS dendrimer-functionalized APTES-modified Fe$_3$O$_4$@SiO$_2$

DGA-PAMAM-SDB diglycolamic acid terminated polyamidoamine dendrimer functionalized styrene-divinylbenzene chelating resin

Fe$_3$O$_4$/SiO$_2$/PNPEDA-G3-COOH modification of polyamidoamine G3 dendrimer with magnetite core to enrich branched amine groups and peripheral carboxyl groups

Fe$_3$O$_4$/SiO$_2$/thermosensitive/PAMAM-CS Fe$_3$O$_4$/SiO$_2$ nanoparticles modified with polyamidoamine immobilized on chitosan

Fe$_3$O$_4$@HPAMAM hyperbranched polyamidoamine grafting onto the surface of Fe$_3$O$_4$ nanoparticles

Fe$_3$O$_4$@PAMAM polyamidoamine dendrimer functionalized with magnetite nanoparticles

Fe$_3$O$_4$@SiO$_2$/GPTMS polyamidoamine generation 6 (PAMAM-G6) dendrimer functionalized Fe$_3$O$_4$/SiO$_2$ nanoparticles

Fe$_3$O$_4$@SiO$_2$-G2.0-S schiff base decorated PAMAM dendrimer/-magnetic Fe$_3$O$_4$ composites

Fe$_3$O$_4$@SiO$_2$-M2 sulfur-functionalized polyamidoamine dendrimer/magnetic Fe$_3$O$_4$

G2.0-PAMAM-ATP polyamidoamine dendrimers modified attapulgite sorbents

G2.5 PAMAM-coated ultrafiltration membranes polyamidoamine dendrimer modifying ultrafiltration membranes

G-3 PAMAMSGA generation-3 polyamidoamine dendrimer implanted on silica

G3PDFSH polyamidoamine dendrimer functionalized soy hull

G3-PS-GMA polyamidoamine dendrimers generation 3 onto polystyrene-divinylbenzene-glycidyl methacrylate) beads

GO/PAMAMs polyamidoamine dendrimers modifying graphene oxide

Hal-PAMAM dunino halloysite functionalized with polyamidoamine dendrimer

HNTs-(DEN-NH$_2$) halloysite nanotubes functionalized with polyamidoamine dendritic polymers

HNTs-G3 halloysite nanotubes modified with poly (amidoamine) generation 3 dendrimers

M@PAMAM/RSA magnetite nanoparticles immobilized into polyamidoamine dendrimer/montmorillonite or rice-straw-ash hybrids

mGO2nd-PAMAM polyamidoamine dendrimer grafted magnetic graphene oxide nanosheets

MNP-G3 magnetic nanoparticles modified by third-generation dendrimers

MNPs-G3 polyamidoamine dendrimer-modified magnetic nanoparticles (MNPs)

MWCNT-PAMAMG1 polyamidoamine dendrimer functionalized carbon nanotube

NCC-G2 polyamidoamine dendrimer-functionalized nanocrystalline cellulose

NH$_2$-Pal-G4 polyamidoamine dendrimer-functionalized palygorskite

PAMAM grafted PAN-DETA nanofiber polyamidoamine grafted polyacrylonitrile-DETA nanofiber

PAMAM/CNT nanocomposite carbon nanotube coated polyamidoamine dendrimer

PAMAM@GTA-NH$_2$-MSF polyamidoamine dendrimer immobilized on mesoporous silica foam

PAMAM@GTA-NH$_2$-KCC-1 polyamidoamine dendrimer immobilized on fibrous nano-silica KCC-1

PAMAMG3-Fe$_3$O$_4$/P(GMA-AA-MMA) polyamidoamine dendron functionalized superparamagnetic polymer microspheres

PAMAM–SDB polyamidoamine dendron grafted styrene-divinylbenzene chelating resins

DGA–PAMAM–SDB diglycolamide functionalized polyamidoamine dendron grafted styrene-divinylbenzene chelating resins

PAN/PAMAM composite nanofibers polyacrylonitrile nanofibers modified with polyamidoamine

PAO-h-PAMAM hyperbranched polyamidoamine-modified polyacrylonitrile fibres hyperbranched polyamidoamine and amidoxime groups

PDMAEMA polyamidoamine dendrimer modified styrene core

PVDF-g-PAA-G3.0 PAMAM membrane different generation polyamide-amine grafted onto PVDF-g-PAA membranes

SBA-15/PAMAM mesoporous SBA-15 functionalized with polyamidoamine dendrimer

SG-DETA and SG-DETA2 silica-gel-based adsorbents grafting of dendrimer-like highly branched polymer

SG-G2.5 polyamidoamine dendrimers functionalized silica

SG-MITC-G2.0 silica gel supported sulfur-capped polyamidoamine dendrimers

Si-6G PAMAM polyamidoamine dendrimers modified silica gel

SiO$_2$-G1.0 polyamidoamine dendrimer/silica gel

SiO$_2$-G2.0-SA Schiff base functionalized polyamidoamine dendrimer/silica

SiO$_2$–PAMAM(4) silica-based hybrid materials functionalized with polyamidoamine dendrimers

1. Introduction

Branched architectures occur naturally in tree roots, broccoli, blood vessels, and nerve cells. In chemistry, the first representative report of similar structures was provided by the Vögtle group in 1978 [1]. Using a series of primary monoamines and diamines, a "cascade synthesis" approach was used to attach spacer units of propylenamine where the N atoms served as branching points across every repetitive synthetic step. Since its inception, "cascade molecules" have evolved as lucrative systems for multiple applications in nuclear medicine [2,3] and environmental remediation [4,5].

The term dendrimers became popular in 1980 replacing the name "cascade molecules". The name dendrimer is derived from the Greek words *dendron* (tree) and *meros* (part) being extensively used to name tree-like branched compounds. Dendrimers are defined as molecular architectures of perfectly defined size and terminal groups. The branches are successively constructed from a core unit order as regular layers in three-dimension from inside outwards [6]. The so-called generations are used for referring to the molecular size of a specific type of dendrimer. Each branched structure starting from the central unit is called dendron. The surface (also known as the periphery) of the dendrimer is constituted by the end or terminal functional groups. The physicochemical properties of the dendrimer such as shape, conformational rigidity/flexibility, solubility, stability, and viscosity are closely related to the nature of the terminal groups. The number of terminal functionalities is related to the dendrimer generation with higher the dendrimer generation, more are the number of end groups [6,7].

There are two common approaches reported in the literature for the preparation of dendritic polymers: the divergent (or inside out) method and the convergent (or outside in) method. The divergent methodology starts from the core and growing up the polymer through the coupling of the monomer and the activation (transformation or deprotection) of the terminal functional groups. Meanwhile, the convergent route starts from the surface to the core. The inside out method is preferred over the outside in because it allows faster growth of the dendrimer with an increase in the mass of isolated products without significant steric inhibition at early generations [8].

Polyamidoamine (PAMAM) is one of the most extensively studied dendrimers due to its low cost, low toxicity, and easy fabrication (Fig. 1**A**). The PAMAM branched structure was first reported by Tomalia and co-workers in 1985. The preparation procedure consisted of the reaction of methyl acrylate with ammonia (Michael addition). The obtained ester was treated with an excess of ethylenediamine to convert it into a primary triamine (Fig. 1**B**). Through repetition of the reaction sequence, dendrimers up to the 10th generation were reported [9,10]. The versatility of this polymer allows the preparation using other amines and silanols as the core.

Water pollution and increasing demand for clean water for the growing world population have brought the need for developing efficient strategies for water remediation. In that regard, PAMAM-based adsorbents have gained attention for water purification as adsorbents and detection and quantification of toxic pollutants as sensors. Moreover, PAMAM-based materials are being used for CO_2 capture and conversion technology, which is required to curb global warming and associated environmental damages. This review provides an overview of the preparation of PAMAM-based adsorbents using a wide variety of supports to either grow or immobilize the dendrimer. The physicochemical properties involved in their adsorptive properties are highlighted. The adsorption mechanisms of a wide variety of pollutants (cationic and anionic pollutants, precious metals, radionuclides, CO_2) (Table 1) and the applications as sensors are discussed in various subsections of the review (Fig. 2). Finally, some considerations on the PAMAM toxicity and environmental concerns have been discussed with a focus on its judicious use.

2. Fabrication of PAMAM-adsorbents

PAMAM is known for presenting a great variety of end groups along with easy surface engineering, allowing its use for environmental remediation. Despite the effectiveness of these polymers for removing a large variety of pollutants (metal ions, radionuclides, dyes, drugs, and pesticides), their recovery from the aqueous phase is difficult. Therefore, the most effective strategy is to grow or immobilize the dendrimers onto a variety of solid supports (Fig. 3**A&C**). Magnetite nanoparticles are among the most attractive supports due to their low cost, biocompatibility, easy preparation, low environmental toxicity, and magnetic properties. On the other hand, carbonaceous materials such as graphene oxide, carbon nanotubes have been employed as supports for growing or immobilizing dendrimers and improving the adsorptive properties of PAMAM-based hybrid materials. The following subsections deal with the most used and recent approaches to immobilize PAMAM dendrimers onto magnetic and non-magnetic supports (Fig. 3**B**).

2.1. Magnetic supports

The use of magnetite nanoparticles as support is a popular strategy to develop reusable magnetic adsorbents for environmental remediation [11–14]. In that regard, PAMAM-based materials have been developed using magnetic nanoparticles as support, either for growing or anchoring the dendrimer such that the end groups of the polymer are exposed to ensure a stronger interaction with the target pollutant. In general terms, the growth of PAMAM dendrimers on the surface of magnetite nanoparticles is carried out through a series of steps: (a) preparation of the magnetic support, (b) functionalization of the support and (c) the growth of dendritic
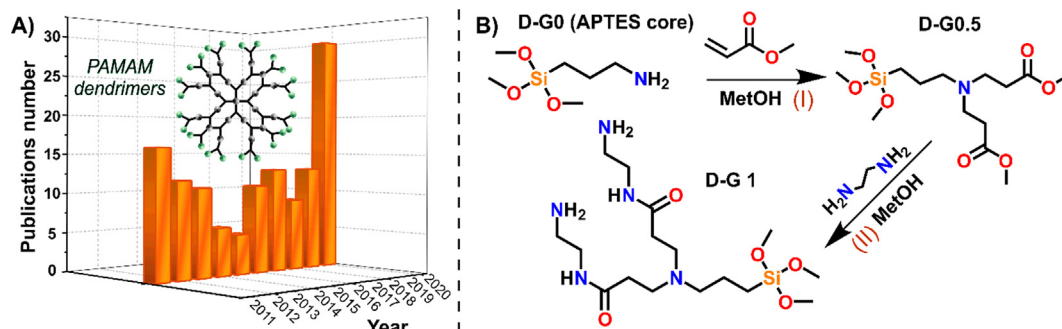

Fig. 1. (**A**) Number of PAMAM related research articles in the last decade (Web of Science); (**B**) First PAMAM generation preparation using 3-aminopropyl(trimethoxysilane) (APTES) as reaction core through Michael's addition (I) and amidation reaction (II).

Table 1
Dendrimer-based adsorbents for pollutant removal.

Adsorbents	Pollutant	Experimental conditions				%Removal efficiency/ Q_{max} (mg g^{-1})
		pH	Time (min)	Dosage (g L^{-1})	C (mg L^{-1})	
Alg/Hal_PAMAM beads [27]	Methyl green	7	1440	2.5	200	97.0/113.6
CCMD [59]	Methylene blue	11	240	1.5	100	–/96.3
Fe$_3$O$_4$@SiO$_2$-G2.0-S [19]	Hg(II)	6	180	1.2	802	–/605.8
DF-MNS [53]	Hg(II)	6.5	5	0.5	20	–/90.0
G2.0-PAMAM-ATP [29]	Hg(II)	5	80	5	120	–/248.1
CT-HPMNPs [18]	Hg(II)	5	60	2	20	–/72.3
G-3 PAMAM-SGA [100]	Cd(II)	5	180	1	125	–/24.5
SG-G2.5 [50]	Cd(II)	6	200	1	562	–/216.9
CS-G3 [48]	Pb(II)	6	240	0.1	500	–/44.0
PVDF-g-PAA-G3.0 PAMAM membrane [58]	Cu(II)	–	–	–	200	–/101.0
NCC-G2 [49]	Cu(II)	5	1440	0.2	500	–/92.1
SG-G2.5 [51]	Cr(III)	4	180	1	260	–/26.5
mGO2nd-PAMAM [55]	Cd(II)	7	90	0.06	30	–/435.8
	Pb(II)	6		0.05	20	–/326.7
	Cu(II)	7		0.05	20	–/353.6
SiO$_2$-G2.0-SA [52]	Mn(II)	4	120	–	–	–/50.5
	Co(II)	6				–/55.4
PAMAM/CNT [23]	Co(II)	7	30	0.03	100	–/494.0
	Zn(II)					–/470.0
PAMAM/CNT [56]	Cu(II)	7	–	0.03	100	–/3677.0
	Pb(II)					–/4080.0
SiO$_2$–PAMAM(4) [25]	Ni(II)	5.4	–	1	880	–/116.6
	Co(II)					–/101.1
	Ca(II)	–	30	0.2	40	–/79.0
Fe$_3$O$_4$/SiO$_2$/PNPEDA-G3-COOH [34]	Cr(II)				52	–/10.4
	Pb(II)				207	–/55.9
	Ni(II)				59	–/62.7
	Cu(II)				64	–/127.5
PAN/PAMAM composite nanofiber [101]	Direct red 80	2.1	60	0.033	40	–/1666.6
	Direct red 23					–/2000.0
PAMAM grafted PAN-DETA nanofiber [102]	Direct red 80	3.5	60	0.033	40	–/3333.3
	Direct red 23					–/2500.0
Amine-functionalized α-Fe$_2$O$_3$ nanofiber [67]	Direct red 80	3	60	–	40	–/1428.6
	Acid red 18					–/1250.0
Alg/Hal_PAMAM beads [27]	Sunset yellow FCF	6	1440	0.0025	60	91.0/–
SBA-15/PAMAM [66]	Acid blue 62	2	60	0.3	40	–/1428.6
GO/PAMAM [68]	Congo red	11	600	0.02	–	–/198.0
HNTs-G3 [103]	C.I. acid red 1	3	60	0.7	25	93.0/–
	C.I. acid red 42			0.5		94.0/–
GO/PAMAMs [104]	Acid Bordeaux B	2.5	400	1	150	–/325.8
NH$_2$-Pal-G4 [105]	Reactive red 3BS	4.5	20	0.2	100	–/322.6
GO/PAMAMs [64]	NO$_3^-$	7.5	15	0.045	25	90.0/–
M@PAMAM/MMT	NO$_3^-$	6	420	1	5	83.0/–
M@PAMAM/RSA [65]	Br$^-$	8	420	1	5	98.0/–
HNTs-(DEN-NH$_2$) [69]	Cr$_2$O$_7^{2-}$	3	60	1	11	98.0/23.6
HNTs-PAMAM (G5) [106]	Cr$_2$O$_7^{2-}$	3	4320	–	58	–/49.3
Fe$_3$O$_4$/SiO$_2$/PNPEDA G3-COOH [34]	Cr$_2$O$_7^{2-}$	–	30	2	294	–/10.4
G3-PS-GMA [28]	Glyphosate	3	5	–	50	95.0/–
PDMAEMA [107]	Glyphosate	7.7	10	–	5	93.0/–
MNPs-G3 [108]	Organochlorine pesticides	7	40	1.33	0.02	91.8–103.5/–
Fe$_3$O$_4$@SiO$_2$/GPTMS [35]	As(III)	7	40	40	5	–/233.0
PAMAM/CNT nanocomposite [23]	AsO$_3^{3-}$	7	30	0.03	100	–/432.0
GO-gen2-Aza [70]	AsO$_3^{3-}$	–	1440	1	0.1	–/80.5
Fe$_3$O$_4$@PAMAM [109]	NSAIDs	7	5	0.5	0.3	93.6–98.9/–
G2.5 PAMAM-coated amidoximated ultrafiltration membranes [74]	Lasalocid A	4	90	–	100	82.5/–
	Salinomycin					87.3/–
	Semduramicin					91.3/–
Fe$_3$O$_4$/SiO$_2$/thermosensitive/PAMAM-CS [17]	Tamoxifen	8	30	–	20	100.0/20.5
Hal-PAMAM [37]	Ibuprofen	6	1440	5	800	–/68.3
	Naproxen				100	–/5.9
PAMAM/SiO$_2$ nanohybrid [4]	Clofibric acid	9	25	0.001	0.1	–/94.0
	Diclofenac					–/134.0
	Ibuprofen					–/124.0
	Ketoprofen					–/112.0
PAO-h-PAMAM [96]	U(VI)	8.3	1440	0.02	20	–/493.6
CTS [98]	Am(III)	5	60	50	–	–/6.0
	Eu(III)					–/6.0
PAMAM-SDB	U(VI)	5.5	120	1	–	95.0/–
	Th(IV)					95.0/–
DGA-PAMAM-SDB [97]	U(VI)					95.0/–
	Th(IV)					95.0/–

Table 1 (continued)

| Adsorbents	Pollutant	Experimental conditions				%Removal efficiency/ Q_{max} (mg g^{-1})
		pH	Time (min)	Dosage (g L^{-1})	C (mg L^{-1})	
DGA-PAMAMG5-SDB [110]	U (VI)	>4	120	1	250	–/682.0
	Th(IV)				100	–/544.2
MWCNT-PAMAMG1	Pu(VI)	–	120	10	–	–/89.2
MWCNT-PAMAMG2 [92]						–/92.5
MWCNT-PAMAMG1	Am(III)	–	120	–	–	–/82.6
MWCNT-PAMAMG2 [94]						–/97.6
MWCNT-PAMAMG1	Np(III)	2	180	5	–	–/56.1
MWCNT-PAMAMG2 [93]						–/58.8
Si-6G PAMAM [95]	U(VI)	4.5	60	1	800	–/303.0
PAMAMG3-Fe$_3$O$_4$/P(GMA-AA-MMA) [38]	U(VI)	4.5	180	0.4	100	98.5/–
PAMAM@GTA-NH$_2$-MSF	Gd(III)	6	360	1	200	–/132
PAMAM@GTA-NH2-KCC-1 [99]						–/88.7
G3PDFSH [111]	La(III)	–	240	1	60	67.0/–
	Nd(III)					52.0/–
	Sm(III)					35.0/–
SG-MITC-G0	Ag(I)	6	270	1.0	215	–/129.6
SG-MITC-G1.0						–/129.6
SG-MITC-G2.0 [84]						–/140.4
Fe$_3$O$_4$@SiO$_2$-M2	Ag(I)	6	600	2.5	200	–/139.3
Fe$_3$O$_4$@SiO$_2$-M1						–/130.7
Fe$_3$O$_4$@SiO$_2$-M0 [82]						–/113.4
SG-DETA	Au(III)	2	720	2.5	478.0	–/411.7
SG-DETA2 [83]						–/417.6
MNP-G3 [79]	Pd(IV)	6.5	–	5.0	20	–/3.6
	Au(III)					–/3.6
	Pd(II)					–/2.7
	Ag(I)					–/2.8
NSAIDs: Non-steroidal anti-inflammatory drugs						
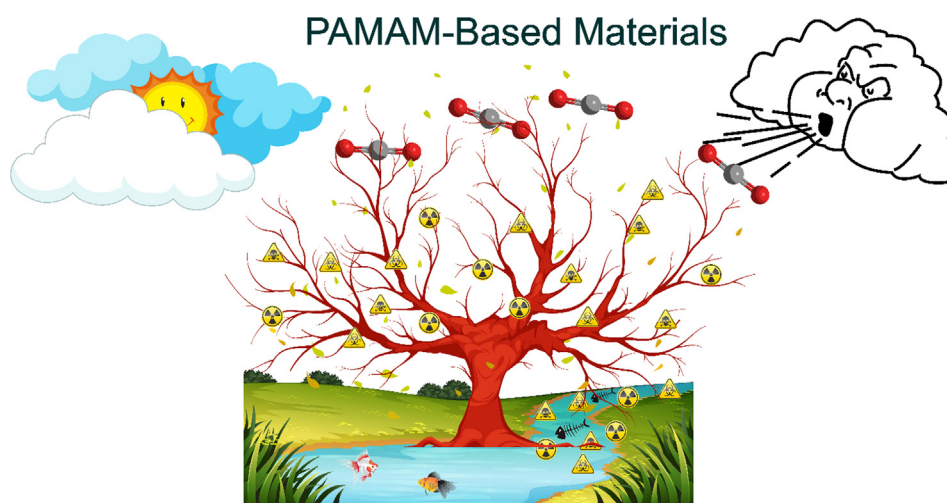
Fig. 2. Graphical representation of PAMAM-based materials for environmental applications.

architecture. Zarei and co-workers developed Fe$_3$O$_4$@SiO$_2$@-carboxyl-terminated PAMAM dendrimer nanocomposite. The first step was the preparation of magnetic nanomaterial by co-precipitation of iron salts in a basic media. Afterwards, the Fe$_3$O$_4$ nanoparticles were functionalized with a layer of silica using the Stöber method. The as-prepared Fe$_3$O$_4$@SiO$_2$ nanoparticles were modified with NH$_2$ terminals by reacting the nanoparticles with (3-aminopropyl)triethoxysilane. The purified Fe$_3$O$_4$@SiO$_2$-NH$_2$ dispersed in methanol were left to interact with methyl acrylate under a nitrogen atmosphere. The acrylate modified material was washed and re-dispersed in methanol and ethylenediamine and the reaction mixture was stirred to yield the first generation of PAMAM dendrimer over the nanoparticles. The third generation PAMAM dendrimer was grafted using the same sequence of reactions twice, leading to the formation of Fe$_3$O$_4$@SiO$_2$@PAMAM-G3. Finally, the amino terminals were carboxylated by reacting the nanoparticles with monochloroacetic acid for heavy metal capture [15]. Once the dendrimer is grown on the surface of the magnetic core, post-functionalization can be performed to enhanced the affinity of the composite toward the targeted pollutant using other terminal groups such as dithiocarbamate, chitosan, and trimesic acid [16–18].
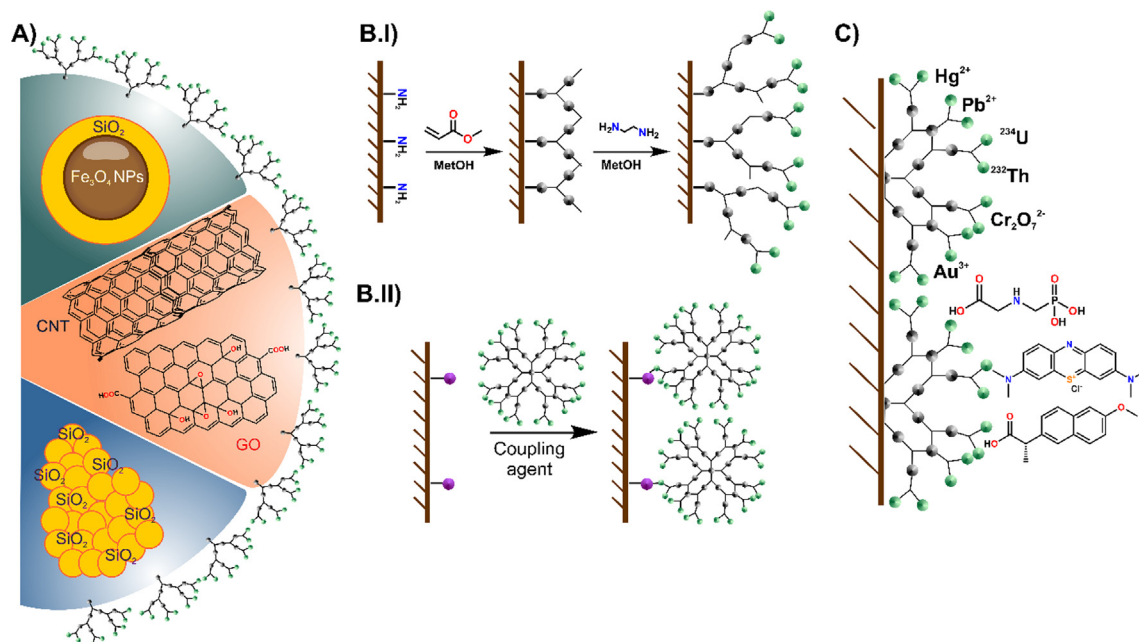
Fig. 3. (**A**) Most common supports for PAMAM immobilization: magnetite nanoparticles coated with silica shell (Fe$_3$O$_4$@SiO$_2$ nanoparticles), carbon nanotubes (CNT), graphene oxide (GO), silica (SiO$_2$); Approaches for support functionalization with PAMAM; (**B.I**) Growing dendrimer generations onto the support surface; (**B.II**) Coupling of the functionalized support with PAMAM using a coupling reagent; (**C**) Removal of metal ions, anions, radionuclides, dyes, drugs, and pesticides using PAMAM-based adsorbents.

The other commonly used strategy to prepare magnetic PAMAM-based adsorbents is the grafting of PAMAM generations on the surface of the magnetite nanoparticles. Zhou and co-workers reported the preparation of Schiff base decorated PAMAM dendrimers/magnetic composites by grafting the PAMAM dendrimers on the surface of the magnetic core and further functionalization with salicylaldehyde to yield the Schiff base on the periphery of the dendrimer. Different PAMAM generations (G0.5-G2.0) were prepared separately under a nitrogen atmosphere using the repetitive Michael addition and amidation reactions to obtain G1 and G2. The PAMAM grafted magnetic nanoparticles were prepared by dispersing synthesized Fe$_3$O$_4$@SiO$_2$ nanoparticles and G1 or G2 dendrimer in toluene. The reaction to decorate PAMAM terminals with Schiff bases was carried out by dispersing the PAMAM coated Fe$_3$O$_4$@SiO$_2$ nanoparticles and salicylaldehyde in anhydrous ethanol. The suspension was refluxed under sonication to allow the reaction between the amino terminals of G1 or G2 and the aldehyde group. The final adsorbents were tested for mercury removal [19].

2.2. Non-magnetic supports

The growth or immobilization of PAMAM dendrimers to achieve functional adsorbents have been carried out using non-magnetic supports. Moreover, the conjugation of carbonaceous or silica supports with dendrimers has equally produced highly effective materials, but with a low adsorbent recovery.

2.2.1. Carbonaceous supports

The use of carbonaceous supports to prepare dendritic based adsorbents results in materials with a larger surface area and enhanced sorption capacities due to adsorptive properties of carbonaceous materials and functionalities of the grafted PAMAM terminals. Graphene oxide (GO) and carbon nanotubes (CNTs) are commonly used as support for dendrimers. Zhang and coworkers developed a graphene oxide/PAMAM adsorbent through a "grafting to" procedure, obtaining a highly effective adsorbent for metal ions removal. In this strategy, as prepared GO and PAMAM were

mixed to achieve the final composite. First, GO was prepared by a variant of the Hummer method. Next, the G2 PAMAM was prepared by repeating the sequence of Michael addition and the amidation reaction using ethylenediamine. To prepare the PAMAM-modified GO, a solution of PAMAM-G2 in absolute methanol was added to the DMF solution of GO under stirring. The grafting was possible due to the reaction of GO functionalities (—OH and —COOH) with the amino groups of PAMAM periphery [20].

Another approach to achieve GO modified with PAMAM dendrimers is the step-by-step growth of PAMAM onto the GO surface. This procedure was first reported by Xiao et al. obtaining PAMAM-GO with different generations of PAMAM on the GO surface for selenium ions removal. First, the graphene oxide was prepared by a variation of the Hummer method. The as-prepared GO with O-bearing surface functionalities (hydroxyl, carboxyl, and carbonyl groups) was allowed to react with (3-aminopropyl)triethoxysilane. This yielded amine-functionalized GO, denoted as GO-G0. Then, the growth of different PAMAM generations was carried out over GO-G0 by repetitive Michael addition followed by amidation reactions to produce GO with G1, G2, G3, and G4 dendrimers [21].

CNTs are attractive support for PAMAM functionalization and different strategies have been proposed for the same. A simple coupling process of modified CNT with PAMAM dendrimer was proposed by Hayati et al. PAMAM generations from one to five were prepared by the sequence of Michael addition and amide reaction with ethylenediamine. Then, the coupling reaction was carried out with the modified CNT. First, CNTs were oxidized in acid media to obtain CNT-COOH. It was followed by the addition of N-hydroxysuccinimide and N-ethyl-N-(3-dimethylamino propyl) carbodiimide hydrochloride to the pre-homogenized CNT-COOH in water. Finally, a dendrimer solution in ethanol was added and the reaction mixture was kept under stirring to achieve the covalent coupling of the PAMAM onto the CNT surface [22].

Hayati and coworkers reported another strategy to obtain PAMAM-modified CNTs by growing the dendrimer on the surface of the carbon nanotubes instead of coupling it. For this, the oxidation step of the CNT was performed with some variations. The oxidized

nanotubes were reacted with $SOCl_2$ to obtained CNT-COCl. Then, CNT-COCl was dispersed in tetrahydrofuran under sonication and treated with an excess of ethylenediamine. The modified CNTs were treated with methylmethacrylate to obtain the ester terminal and further addition of ethylenediamine resulted in the PAMAM-modified CNTs [23].

2.2.1.1. Silica supports. Functionalized silica adsorbents have been widely used for the removal and recovery of pollutants and therefore its modifications using PAMAM is another popular strategy for developing efficient materials for wastewater treatment. Niu *et al.* reported the preparation of silica gel supported salicylaldehyde modified PAMAM dendrimers as an adsorbent for mercury ions. The first step involved the activation of the silica-gel with γ-amino propyltriethoxysilane yielding the aminated silica, SiO_2-G0. PAMAM dendrimers (G1 or G2) were grown through the conventional approach over the SiO_2-G0, yielding SiO_2-G1 and SiO_2-G2. Next, the coupling of the PAMAM-modified silica with salicylaldehyde was carried out. The general procedure for the modification with the aldehyde was mixing the SiO_2-G1 or SiO_2-G2 and salicylaldehyde in ethanol and refluxing the solution in a nitrogen atmosphere. The reaction time was dependent on the dendrimer generation with G2 taking more reaction time [24]. Santa Barbara Amorphous-15 (SBA-15) is a highly stable mesoporous silica with high hydrothermal and mechanical stability which has found diverse environmental applications. Mirzaie *et al.* reported the preparation of SBA-15/PAMAM adsorbent for dye capture. The SBA-15 was prepared by the conventional method and further modified with —Cl functionalities. Finally, the —Cl functionalities were replaced by the commercially available PAMAM G0 yielding SBA-15/PAMAM [5].

Recently, four silica-PAMAM hybrid materials were prepared by the grafting of PAMAM dendrimers with different amino-terminal groups for superior removal of Ni(II) and Co(II). The PAMAM dendrimers were prepared using tris(2-aminoethyl)amine as the amine core. The first step consisted of the Michael addition between methyl acrylate and the amino core. Next, the amidation reaction was carried out using four different amines: ethylenediamine, tris(2-aminoethyl)amine, triethylenetetramine, and 4,7,10-trioxa-1,13-tridecaneamine. Next, the silica material was modified using the dendrimers. For this, silica-gel functionalized with the isocyanate groups was slowly added to a solution of the dendrimer in anhydrous methanol. The reaction of the free amino terminals of dendrimers with the isocyanate groups from the silica led to the formation of hybrid adsorbents [25]. It is worth noticing that many solid supports have been used for the preparation of PAMAM-functionalized adsorbents. In that regard, clays, polymer fibres, and commercial membranes are more recent choices to either grow or graft the PAMAM dendrimers [26–30]. A thorough revision of the use of these supports is out of the scope of the present review.

3. Physicochemical properties

The application of PAMAM-based materials in wastewater treatment and CO_2 capture is highly dependent on the type of functionality, degree of functionalization, and the generation of PAMAM dendrimers [31,32]. The modification of PAMAM terminal groups depends on the final application with the amine, carboxyl, and hydroxyl groups being the most used functionalities for the adsorption process [32]. The properties of dendrimer such as highly-branched three-dimensional shape, accessible internal cavities, degree of functionalization, and surface charge are key factors to develop a suitable dendritic structure for environmental remediation. Dendrimers are characterized using conventional microscopic and spectroscopic techniques to evaluate their physicochemical properties.

The three-dimensional configuration of dendrimer gives them superior properties compared to the linear polymers. Their hyper-branched globular shape, which consists of a multifunctional architecture and empty internal cavities, improves the interaction between dendrimers and contaminants [31]. The morphology and size of dendrimer particles can be studied by scanning electron microscopy (SEM). In most cases, PAMAN dendrimers have a spherical or hexagonal morphology [4,35,36]. Zhou *et al.* observed spherical microstructures of PAMAN gel particles interconnected due to intermolecular cross-linking, which resulted in the formation of voids (Fig. 4**A**) [33]. These voids or empty cavities increase the adsorption capacity of the dendritic structure.

When inorganic materials such as halloysite, magnetite, and quartz are functionalized with PAMAN dendrimers, powder X-ray diffraction pattern (PXRD) should be recorded to determine the structural stability of the material after the process. An insignificant change in the PXRD patterns indicates excellent stability of the material after the organic functionalization [36–38]. Lakshmi *et al.* studied the possible crystallinity change in magnetite nanoparticles after functionalization with SiO_2 and PAMAM dendrimers [34]. After the dendrimer incorporation, all characteristic peaks of the magnetite phase were intact with peak broadening arising probably from a loss in the crystallinity (Fig. 4**B**). Though the grafting of PAMAM over the support cannot be probed by the PXRD analysis, it does give information on the structural stability of the PAMAM-based materials. The surface area and porosity of supports are expected to change with the degree of PAMAM functionalization. N_2 adsorption-desorption isotherm at 77 K is recorded and the surface area is calculated by Brunauer-Emmett-Teller method (BET) method. Lotfi *et al.* [4] and Zhou *et al.* [19] found that the pore volume of SiO_2 and Fe_3O_4@SiO_2 decreased significantly after PAMAM grafting. The decreased pore volume is expected due to the blocking of external pores by the bulky PAMAM dendrimer units (Fig. 4**C**).

Fourier Transform infrared spectroscopy (FT-IR) and X-ray photoelectron spectroscopy (XPS) are exploited to monitor functionalities and degree of functionalization in PAMAM-based adsorbents. The modification of Fe_3O_4@SiO_2 with Schiff base decorated PAMAM dendrimer (G0.5-G2.0) can be probed by FT-IR spectroscopy where the peak at 1740 cm^{-1} in G0.5 represented the stretching vibration of the ester carbonyl group. After adding ethylenediamine, the signal at 1740 cm^{-1} for G0.5 disappeared with the origin of amide groups (at 1540 and 1640 cm^{-1}), confirming the synthesis of G1.0 (Fig. 4**D**).

Surface-sensitive techniques have become an interesting tool to study the structure and composition of organic coating layers. XPS analysis is an effective technique for polymer surface analysis since it provides useful chemical information including the presence of functional groups and interfacial interactions of different dendron generations. Viltres *et al.* employed this surface technique for following the PAMAM dendron growth from generation 0 till 4.1 [39]. The core employed for the synthesis of these dendrons was (3-aminopropyl)trimethoxysilane where the alkoxysilane core improves dendron grafting on hydroxylated surfaces. In the case of G4 PAMAM dendron, its N 1s high-resolution spectrum (Fig. 5**A.1**) fitted with three component peaks centred at 399.4 eV (primary and tertiary amine (R = C—N) groups), 399.8 eV (amide (N—C=O) groups belonging to the dendron structure) and 401.6 eV. The small contribution at higher binding energy was due to the amine nitrogen atoms bearing a partial or net positive charge arising either due to the inter and intra-molecular hydrogen bonding or the protonation of amines by water traces. Meanwhile, from the O 1s spectrum, the presence of carboxyl (in the amide group of PAMAM) can be traced at 531.1 eV (Fig. 5**A.2**). The absence of peak above 533.0 eV (O—C=O
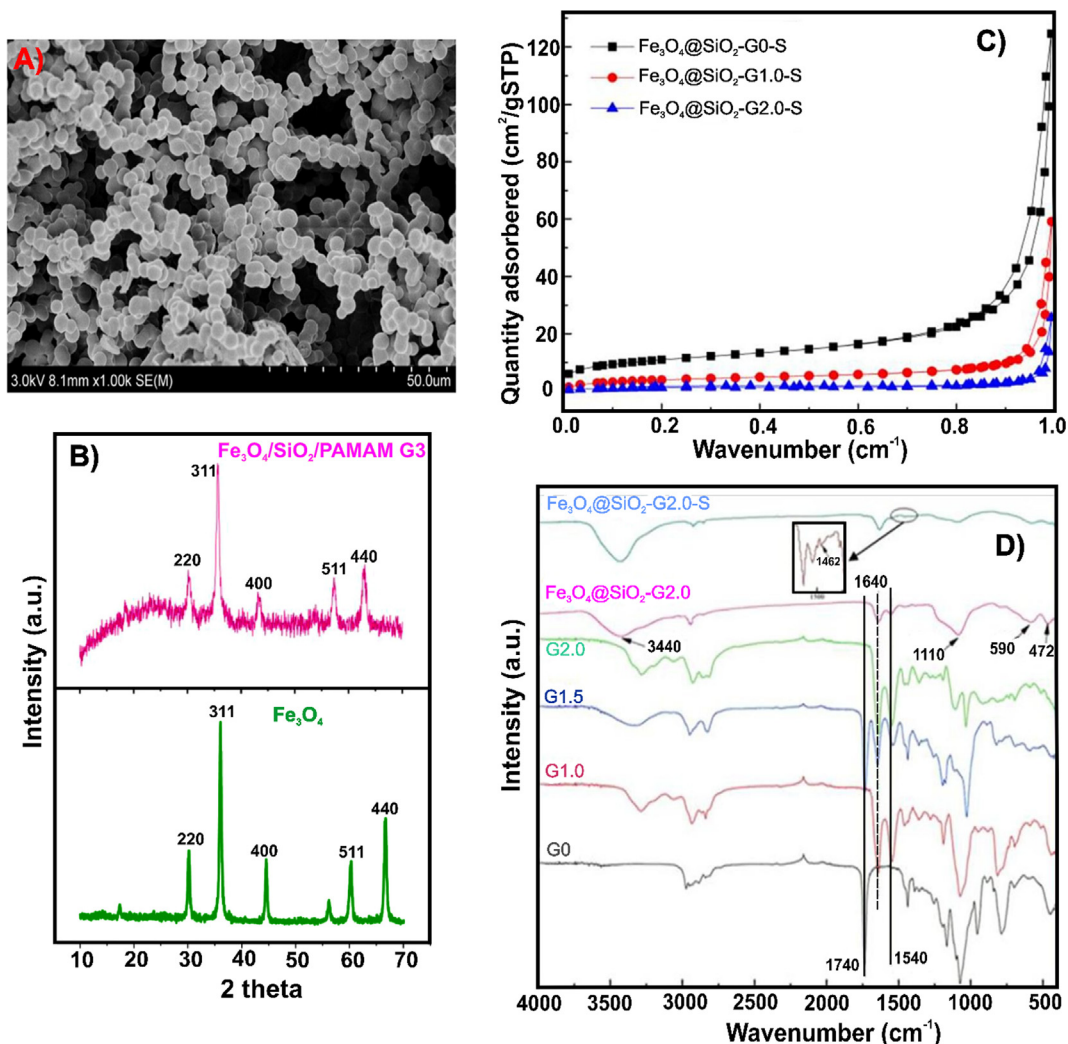
Fig. 4. (**A**) Low-magnification SEM image of PAMAM gel [33]; (**B**) PXRD patterns of Fe_3O_4 and $Fe_3O_4/SiO_2/PAMAM$ G3 [34]; (**C**) N_2 sorption isotherms of $Fe_3O_4@SiO_2$ modified with different PAMAM dendrimer generations [19]; (**D**) FTIR spectra of dendrimers (generation 0–2.0) and after $Fe_3O_4@SiO_2$ modification with G2 dendrimers [19]. (Reproduced with permission from Elsevier 2021).

groups) confirmed the absence of ester groups, which is an indication of dendron formation. Also, the C 1s spectrum confirmed the presence of C—O and C—N and amide carbon in —NH—C=O groups (Fig. 5**A.3**).

The surface charge of the end groups of dendrimers influences the adsorption process. Zeta potential can be understood as the potential difference between the stationary layer of fluid close to the dispersed particle surface and the dispersion medium. Conventional PAMAN dendrimers present tertiary and primary amine terminal groups with a pKa in the range of 6.3–6.9 and 9.3–9.8 respectively [41]. According to pKa values, at pH below 6.9, all amine groups are protonated resulting in positive zeta potential values. As pH increases, the tertiary amine groups begin to deprotonate changing the zeta potential. A study conducted by Tokarczyk and coworkers evaluated the zeta potential value of G4 PAMAM under different ionic strength conditions [40]. As observed in Fig. 5**B**, the zeta potential was positive in the pH 3–8 and dropped in the 8–11 range. Consequently, the net surface charge is positive below pH 10.4 and negative above this value. The G4 PAMAM polymer has 64 surface primary and 62 tertiary amine groups, which are responsible for controlling the protonation-deprotonation mechanism. Under acidic conditions, both amine groups are protonated, while at neutral pH only primary amines

are protonated and pH above 10, both amine groups are deprotonated [40]. Thus, the interaction of cationic or anionic pollutant species with the functionalities of PAMAM dendrimers is highly dependent on the pH of the solution.

4. Environmental applications

4.1. Removal of cationic pollutants

Heavy metal ions and cationic dyes are the most abundant pollutants in wastewater. Toxic metallic ions such as Zn(II), Cu(II), Pb (II), Ni(II), Cd(II), Hg(II) are introduced into water bodies as a result of industrial activities such as mining and metallurgy, fossil fuel production, battery, and plastics manufacturing [42,43]. The rapid industrialization has increased the presence of heavy metal ions in water ecosystems. Furthermore, these pollutants are non-biodegradable and easily accumulate in living tissues, which disrupts cellular metabolism. In some cases, chronic exposure to these pollutants eventually leads to death [22]. Cationic dyes present basic properties in aqueous solution with high-water solubility. The discharge of poorly treated wastewater from textiles, cosmetics, food, plastic, and ceramic industries is responsible for the
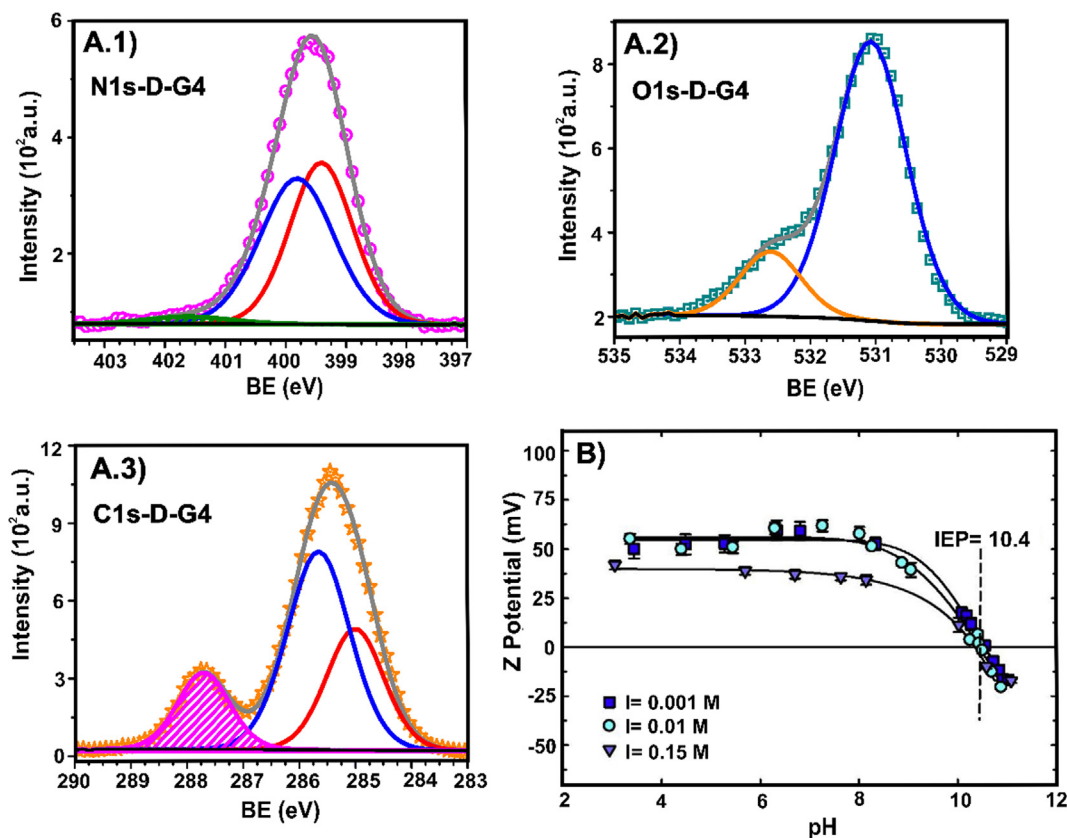
Fig. 5. (**A**) N1s, O1s and C1s High-resolution spectra for PAMAM dendron generation 4 (DG4) [39] (Reproduced with permission from Wiley 2021); (**B**) Dependence of the G4 PAMAM dendrimer zeta potential on pH at ionic strength [40] (Reproduced with permission from Elsevier 2021).

incorporation of these pollutants into the environment [44]. These pollutants are well-known for their high chemical stability, non-biodegradability, and mobility in water. Moreover, the presence of dyes in aquatic ecosystems inhibits the photosynthesis, causing critical damage to marine life. Human exposure to organic dyes can cause allergies, mutagenic, and carcinogenic effects [27,42,45].

Development of new materials for efficient removal of cationic pollutants (heavy metal ions and cationic dyes) is an urgent need. The use of materials based on dendrimers for wastewater treatment has gained importance due to their versatility in size, easy functionalization, low toxicity, and relatively low cost. In that sense, PAMAM dendrimers have been extensively used due to their three-dimensional structure loaded with amino and carboxyl functional groups. Carboxyl functionalities act as a complexing agent and exhibit a high affinity for positively charged pollutants [46,47]. This subsection presents a brief overview of the recent reports on the application of PAMAM dendrimers-based materials for the removal of cationic pollutants from wastewater.

Zarghami *et al.* successfully synthesized a series of integrated bioadsorbents from PAMAM-grafted chitosan and evaluated their capacity as adsorbents for Pb(II) removal. It was found that materials functionalized with the higher PAMAM generation exhibited better adsorption capacities. The G3 PAMAM-grafted chitosan (CS-G3) showed a maximum adsorption capacity of 44.0 mg g^{-1} of Pb(II) ions after 4 h at pH 6. The adsorption occurred through the interaction of Pb(II) ions with the amine groups on the periphery of the dendron [48]. Wang *et al.* prepared a series of nanocrystalline cellulose composites (NCC) functionalized with different PAMAM generations (G1 to G4) as adsorbents for Cu(II) ions removal. The study reported that the higher generation dendrimer on the composites did not necessarily yield the best adsorbents. The material NCC-G2 exhibited the best performance for Cu(II)

removal with a maximum capacity of 92.1 mg g^{-1}. NCC-G3 and NCC-G4 showed lower removal capacity due to steric hindrances arising from the bulky dendritic architecture. The PAMAM modified cellulose presents amide functionalities as well as primary and tertiary amine groups, which were responsible for the complexation of Cu(II) ions. However, computational studies revealed preferential complexation of Cu(II) with the nitrogen of the tertiary amine and O-bearing functionalities [49].

Siliceous materials have been widely used as adsorbents due to their thermal stability, high specific surface area, and good surface functionality. Ren and coworkers prepared a series of PAMAM-dendrimer grafted silica-gel (SG-G0 to SG-G4.0) and evaluated their capacity to remove Cd(II) from water. The study included the adsorbents grafted with the ester-terminated (SG-G0.5, SG-G1.5, SG-G2.5, SG-G3.5) and the amino-terminated (SG-G0; SG-G1, SG-G2; SG-G3; SG-G4) PAMAM. The adsorption was independent of dendrimer generation with SG-G2.0 and SG-G2.5 presented the highest adsorption capacity of 122.5 and 132.6 mg g^{-1}, respectively. Also, the ester-terminated adsorbents exhibited relatively higher adsorption capacity than the corresponding amino-terminated adsorbents. Computational and FTIR analysis confirmed Cd(II) complexation with the amino and carbonyl groups of the adsorbent [50]. In another study, the same research group tested these materials for Cr(III) adsorption, obtaining similar results. The materials SG2.5 and SG2.0 showed the highest adsorption capacities of 26.5 and 25.5 mg g^{-1}, respectively, with the involvement of amine and carbonyl groups in the adsorption process. The DFT calculations suggested the formation of tetra-coordinated Cr(III) complex involving carbonyl oxygen and secondary amine nitrogen for the ester-terminated adsorbents. For amino-terminated adsorbents, *hexa*-coordinated complex formed by carbonyl oxygen, primary and secondary amine nitrogen atoms [51].

Qiao *et al.* prepared PAMAM-silica materials modified with salicylaldehyde via Schiff base formation. The resulting adsorbent was tested for Mn(II) and Co(II) removal. The Mn(II) adsorption capacity increased with the increase in dendrimer generation (SiO_2-G0-SA < SiO_2-G1.0-SA < SiO_2-G2.0-SA). However, in the case of Co(II) adsorption, the materials did not follow the same trend (SiO_2-G0-SA < SiO_2-G2.0-SA < SiO_2-G1.0-SA), suggesting a greater affinity of the peripheral salicylaldehyde groups for Co(II) ions rather than for Mn(II) ions. The interaction between adsorbent and metal ions was studied by DFT using the branching unit of SiO_2-G1.0-SA as a model. The theoretical studies revealed that the metal ions were adsorbed by the chelation of a metal ion by hydroxyl, carbonyl, tertiary amine, and imino (N) groups [52].

Recently, magnetic PAMAM based materials have gained a lot of attention due to the advantages of a magnetic core, which promotes a robust and easy phase separation. Ghodsi *et al.* reported a novel dendrimer functionalized magnetic nano-adsorbent for efficient removal of Hg(II). The material is based on a magnetic core, magnetite nanoparticles modified with G1 PAMAM functionalized with 2-thiophene carbonyl chloride, resulting in thiophene functionalities on the periphery of the material. The material was successfully tested for Hg(II) removal from an aqueous solution at pH 6.5 with the maximum adsorption capacity of 90.0 mg g^{-1}. The presence of soft N and S functionalities on the adsorbent surface was responsible for the chelation of Hg(II) ions (soft acid) [53]. Similarly, Lakshmi and Rangasamy synthesized magnetic-core silica nanoparticles (Fe_3O_4/SiO_2) grafted with G3 PAMAM dendrimers and further functionalized with carboxyl terminals groups. The proposed adsorbent, Fe_3O_4/SiO_2/PNPEDA-G3-COOH, was evaluated for the adsorption of Cr(IV), Pb(II), Ni(II), and Cu(II). The reduction of amide groups leads to the enrichment of the adsorbent with amino groups and the later functionalization with carboxyl groups on the surface led to the fabrication of a functionality-rich adsorbent. The most likely adsorption mechanism involves the complexation of the metal ions with amine and carboxyl functionalities [34].

Zhou and coworkers developed a series of Schiff base decorated PAMAM dendrimer/magnetic Fe_3O_4 composites by growing G0, G1, and G2 PAMAM and later functionalizing it with salicylaldehyde. The Hg(II) adsorption capacity of $Fe_3O_4@SiO_2$-G2.0-S reached 605.8 mg g^{-1} with 100% selectivity in presence of other heavy metals. Spectroscopic and DFT calculations were used to predict the mercury adsorption mechanism. The FTIR characterization showed the involvement of amide and C=N groups in the Hg(II) adsorption process (Fig. 6**A**). More detailed information was extracted from XPS analysis where the variations observed in the high-resolution O 1s and N 1s spectra confirmed the participation of C—N, C=N, CONH, and —OH functionalities (Fig. 6**B and 6C**). Furthermore, the DFT calculations suggested the formation of an hepta-coordinated complex involving one tertiary amine nitrogen atom, two imino nitrogen atoms, two hydroxyls, and one carbonyl oxygen atom (Fig. 6**D**) [19].

Clays are mineral compounds being used for the removal of water pollutants due to their natural abundance and low cost. Halloysite and attapulgite are phyllosilicates that present tubular structures, large surface area, and structural stability. These characteristics have allowed their use for the adsorption of cationic contaminants [27]. Qin and coworkers developed new adsorbents incorporating G1 to G4 PAMAM on the surface of activated attapulgite for Hg(II) removal. The maximum adsorption capacity of 248.1 mg g^{-1} was achieved for G2.0-PAMAM-ATP, which was higher than raw and other functionalized attapulgite materials reported in the literature. XPS results showed variations in the high-resolution N 1s and O 1s spectra, suggesting the coordination of mercury ions with the N and O atoms [29].

Carbon-derived nanomaterials are of great interest as adsorbents due to their large surface area, versatility, stability, and easy surface functionalization. GO and CNTs are emerging as some of the most promising materials in recent years for wastewater treatment [54]. PAMAM-grafted magnetic GO nanosheets (mGO-PAMAM) were prepared for the removal of Cd(II), Pb(II), and Cu(II) ions. These adsorbents were prepared with G1 and G2 PAMAM. The maximum adsorption capacity of G2-PAMAM/GO was 435.8, 326.7, and 353.6 mg g^{-1} for Cd, Pb, and Cu, respectively. The adsorption studies revealed a complex removal process where physicochemical interactions were responsible for high adsorption capacities [55]. Hayati and coworkers functionalized CNTs with G4 PAMAM dendrimers (PAMAM/CNT) for the removal of heavy metals ions, achieving the maximum adsorption capacity for Cu(II) (3333.0 mg g^{-1}), Pb(II) (4870.0 mg g^{-1}), Zn(II) (4016.0 mg g^{-1}), and Co(II) (4065.0 mg g^{-1}) in batch studies. The outstanding adsorption capacities of PAMAM/CNT nanocomposite was mainly due to its high surface area and presence of terminal amino groups of dendrimers, which chelated cations and encapsulated them via electrostatic interaction, hydrogen bonding, and van der Waals interactions [23,56].

For dynamic studies, functionalized polymeric membranes have been used for the removal of pollutants due to their flexibility, porosity, low cost, and reusability [57]. Different generations (G1.0 to G4.0) of PAMAM-modified polyvinylidene fluoride membranes (PVDF-g-PAA-PAMAM) were prepared by Sun *et al.* The PAMAM dendrimers were grafted onto the surface of the PVDF-g-PAA membranes to increase their hydrophilicity and adsorption capacity for Cu(II) ions. The PVDF-g-PAA-G3.0 PAMAM membrane showed the best adsorption capacity of 101.0 mg g^{-1}. According to the adsorption studies, the Cu(II) ions removal process involved physical adsorption, hydrogen bonding, and chelation through the amino functionalities of the PAMAM. Moreover, this type of membrane can be recycled while maintaining a high adsorption capacity with a regeneration rate of 90% [58].

PAMAM based materials can also be used for extracting cationic dyes. In a recent study, Kim *et al.* synthesized a hybrid material by grafting carboxymethyl-chitosan onto magnetic nanoparticles functionalized with G1 PAMAM dendrimers. Carboxymethyl-chitosan is a chitosan derivative containing active carboxyl, hydroxyl, and amino groups, which make it an amphoteric material. Carboxymethyl chitosan-modified magnetic-cored dendrimers (CCMD) exhibited selective adsorption for cationic dyes at basic pH conditions. Methylene blue was selected as a cationic dye and the maximal adsorption on the CCMD at pH 11 was 96.3 mg g^{-1}. The dye adsorption on the modified material was governed by electrostatic interactions between the cationic dye and the negatively charged groups on the adsorbent surface [59]. Alg/HAL/PAMAM beads were prepared by the encapsulation of PAMAM-halloysite nanotubes in alginate for cationic methyl green removal. The maximum adsorption capacity was 113.6 mg g^{-1} with a removal efficiency of 97%. The study predicted ion-exchange as the main mechanism behind the dye adsorption process. The regenerated adsorbent exhibited satisfactory adsorption efficiency even after six consecutive cycles [27].

4.2. Removal of anionic pollutants

Anionic pollutants like nitrate, anionic dyes, glyphosates, and anionic heavy metal species like chromate, arsenate, and arsenite are key pollutants in wastewater contributed by different industrial and agricultural practices [60]. The extensive use of these chemicals in industrial and agricultural sectors and improper treatment of industrial and urban wastewaters lead to their release and dispersion into water bodies. Presence of these pollutants in water
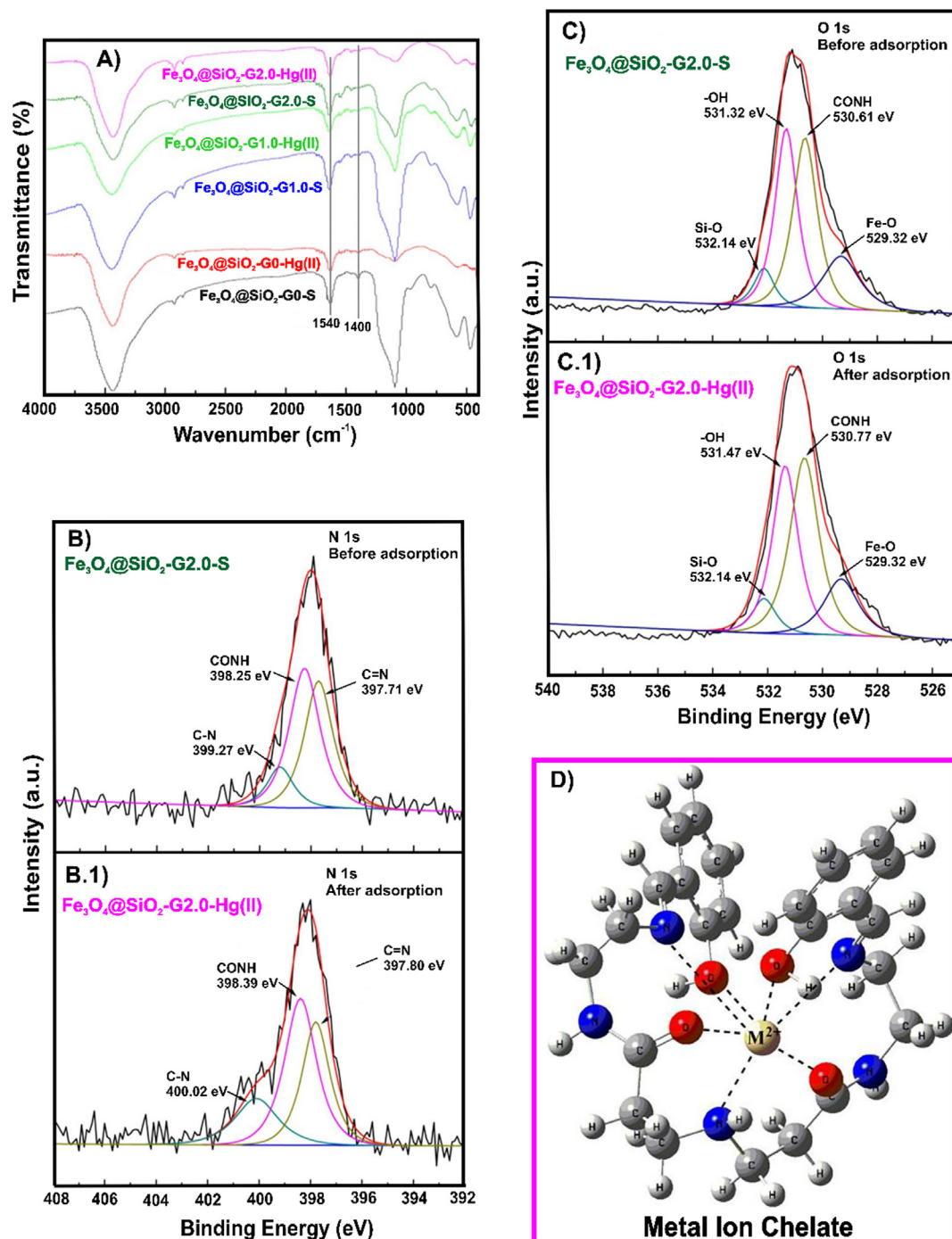
Fig. 6. (**A**) FTIR spectra of PAMAM-based materials before and after Hg(II) adsorption; (**B**) HRXPS N 1s spectra of Fe₃O₄@SiO₂-G2.0S before and after Hg adsorption; (**C**) HRXPS O 1s spectra of Fe₃O₄@SiO₂-G2.0S before and after Hg adsorption; (**D**) Optimized geometry of ligand and its chelates with a metal ion (M = Hg, Cd, Zn, Mn, Co, Cu, and Pb) [19] (Reproduced with permission from Elsevier 2021).

supplies has serious environmental and human health hazards because of their high solubility, bioaccumulation, and poor biodegradability [60,61]. Nitrate is responsible for methemoglobi-naemia in infants (blue-baby syndrome), the formation of carcino-genic nitrosamines, and hypertension [62]. Toxic dyes disrupt aquatic life and induce mutagenic and carcinogenic disorders lead-ing to the dysfunction of kidneys, reproductive system, liver, brain, and central nervous system in humans [61,62]. Human exposure to arsenates could cause peripheral neuropathy, skin cancer, bladder and lung cancer, and peripheral vascular diseases. Also, chromate exposure to living cells is known to have extreme toxicity in

humans and other mammals [62,63]. Adsorption process using PAMAM-based adsorbents is a promising technique to capture anionic pollutants owing to their unique features of tunable struc-ture and high water/chemical stability.

Aboalghasem *et al.* reported HCl-activated GO/PAMAM nanocomposite for nitrate removal. The nanocomposite showed a high removal efficiency (90%) within 15 min at pH 7.5. The mate-rial exhibited good sorption capacities and recyclability with 51% of nitrate removal even after 10 cycles. The adsorption mechanism involved the anion-exchange process where chloride was replaced by the nitrate ions on the adsorbent surface [64]. Hassan and

coworkers immobilized magnetite nanoparticles onto PAMAM/montmorillonite (M@PAMAM/MMT) for nitrate removal. The nanocomposite exhibited 83% removal capacity for NO_3^- ions. The electrostatic interaction between NO_3^- and NH_4^+ species on the PAMAM periphery at pH 6 was responsible for the nitrate removal [65]. PAMAM-based adsorbents have been employed for the removal of pesticides. A novel adsorbent was developed by grafting PAMAM dendrimers onto poly(styrene-divinylbenzene-gl ycidyl methacrylate) beads. The composite successfully removed ~95% of glyphosate from contaminated water. The adsorption mechanism in glyphosate removal involved electrostatic interaction of negatively charged glyphosate with protonated amine groups of PAMAM dendrimers [28].

PAMAM dendrimers could be used for the removal of anionic dyes in acidic conditions. Mirzaie *et al.* designed a hybrid composite composed of mesoporous SBA-15 and PAMAM dendrimer (SBA-15/PAMAM) for the removal of Acid Blue 62. SBA-15/PAMAM showed a maximum adsorption capacity of 1428.6 mg g^{-1} at pH 2 due to electrostatic interactions between the anionic sulfonate groups of dissolved Acid Blue 62 and cationic amino end groups of PAMAM dendrimers [66]. In another research, α-Fe$_2$O$_3$ nanofibers modified with PAMAM dendrimer were explored for Direct Red 80 and Acid Red 18 removal. PAMAM grafted nanofiber showed exceptionally high adsorption capacity of 1428.6 and 1250.0 mg g^{-1} for Direct Red 80 and Acid Red 18, respectively at pH 3 [67]. Mohammad and coworkers studied the adsorption mechanism of Congo Red (CR) dye onto GO/PAMAM composite. GO/PAMAM presented a maximum adsorption capacity of 198.8 mg g^{-1}. The phenolic hydroxyl groups of GO sheets and terminal amine groups of PAMAM dendrimer were the main adsorption sites. The principal groups contributing to the adsorption mechanism of Congo Red onto GO/PAMAM were —OH groups of GO sheets and the protonated —NH$_2$ (—NH$_3^+$) of PAMAM in neutral solutions and —NH$_2$ group of PAMAM and its protonated form (—NH$_3^+$) in alkaline solutions. Dyes adsorption on dendrimer-based adsorbent materials is facilitated by electrostatic attractions, hydrogen bonding, Vander Waals forces, and entrapment of dyes in dendritic architecture. In this specific study, Congo Red molecules interacted with the adsorption sites via hydrogen bonding. First, Congo Red molecules adsorbed on the amine sites and then fully occupied dye molecules diffuse into the internal hydroxyl sites [68].

Halloysite nanotubes functionalized with PAMAM dendritic polymers (HNTs-(DEN-NH$_2$)) successfully removed 98% of chromate from contaminated water, which was significantly higher than the pristine Halloysite nanotubes (23%). The improvement in Cr(VI) removal over the hybrid composite was mainly related to the electrostatic interactions and molecular imprisonment at different pH values (Fig. 7). At pH 3, the adsorption process was mediated by electrostatic interaction between the protonated amine groups and chromate species. At pH > 7, the adsorption process was driven by chromate imprisonment in voids between the terminal amine groups [69]. Akbari *et al.* studied the adsorption of arsenite over G6 PAMAM-functionalized Fe$_3$O$_4$/SiO$_2$ nanoparticles (Fe$_3$O$_4$@SiO$_2$/GPTMS). Fe$_3$O$_4$@SiO$_2$/GPTMS reached a maximum adsorption capacity of 233.0 mg g^{-1} with reusability up to five cycles [35]. Prabhu *et al.* reported a composite fabricated by encapsulating nano ZrO$_2$ over nitrogen-rich azacytosine tethered PAMAM-functionalized graphene oxide (ZrO$_2$@GO-gen2-Aza) for the removal of arsenite species from water. The adsorption capacity reached to 80.54 mg g^{-1} at pH 9.4 with excellent reusability for four cycles. The main adsorption sites involved in the AsO$_3^{3-}$ removal were amino terminals and ZrO$_2$. At pH ~9.4, the ligand-exchange mechanism between the hydroxyl group and AsO$_3^{3-}$ dominated over the adsorbent surface [70].
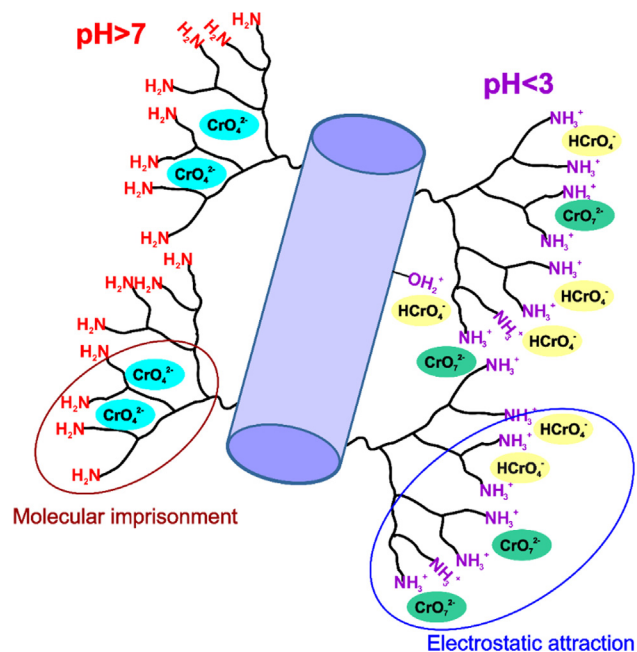

Fig. 7. Cr(VI) removal mechanism by HNTs-(DEN-NH$_2$) at different pH [69].

4.3. Removal of pharmaceuticals

In the last few years, the increase of pharmaceutical compounds in water bodies caused by the continuous release of human and veterinary medicines from domestic sectors and hospitals has become an environmental concern [71,72]. Most of the drugs used in medical treatments can not be processed by the human body and are excreted without significant transformations in their chemical structure and often conjugated to polar molecules, such as glucuronides [71]. Pharmaceuticals are considered as a class of emerging pollutants, which are environmentally persistent due to slow metabolism, leading to toxic effects in aquatic life [71,73]. These contaminants are responsible for endocrine, hormonal, and genetic disorders in living beings. In that regard, the development of novel low-cost and highly efficient adsorbents for removing these new emerging contaminants has been of great importance. To achieve this goal, the use of PAMAM-based adsorbents represents a suitable solution, given an easy surface functionalization of dendritic architectures to capture a large variety of pollutants.

Kurczewska *et al.* studied the removal of ibuprofen and naproxen employing a novel PAMAM-halloysite Dunino (Hal-PAMAM) hybrid as adsorbent. The maximum adsorption capacities of Hal-PAMAM were 68.3 and 6.0 mg g^{-1} for ibuprofen and naproxen, respectively. The adsorption capacity of Hal-PAMAM increased by increasing pH in the range from 3 to 6 [37]. Lofti and co-workers employed a dendritic adsorbent, PAMAM/silica nanohybrid (PAMAM/SiO$_2$) for the adsorption of diverse pharmaceutical pollutants from hospital wastewater. PAMAM/SiO$_2$ showed maximal adsorption capacity of 94.0, 134.0, 124.0, and 112.0 mg g^{-1} for clofibric acid, diclofenac, ibuprofen, and ketoprofen, respectively. Electrostatic interactions were involved in the adsorption process between negatively charged pharmaceuticals and the positively charged PAMAM/SiO$_2$ surface. Also, non-electrostatic interactions took part in the adsorption process based on the solution pH. Non-electrostatic interaction involving hydrogen bonding originated from the interaction of neutral species of acidic pharmaceuticals at pH below the pKa [4].

Fe$_3$O$_4$/SiO$_2$ nanoparticles with core-shell morphology were modified with PAMAM and then the obtained composite was immobilized in chitosan to yield Fe$_3$O$_4$/SiO$_2$/Thermosensitive/PAMAM-CS nanoparticles for the removal of tamoxifen. Fe$_3$O$_4$/SiO$_2$/Thermosensitive/PAMAM-CS nanoparticles showed a maximum adsorption capacity of 20.5 mg g^{-1}. After seven consecutive adsorption/desorption cycles the adsorbent showed an insignificant change in its performance [17].

Cao et al. used PAMAM as a novel antifouling agent and chemically coated on the amidoximated membranes with different half generations (G0-G2.5) for the adsorption of lasalocid A, salinomycin, and semduramicin antibiotics in pharmaceutical wastewater. Membrane surface was modified to reduce the fouling effect (from the formation of cake layer due to the interaction of pollutant with the membrane surface). The G2.5 PAMAM-coated ultrafiltration membrane showed better performance during the filtration process (high water flux and low fouling) than the unmodified membranes. G2.5 PAMAM-coated ultrafiltration membranes could remove 82.5, 87.3, and 91.3% of lasalocid A, salinomycin, and semduramicin antibiotics, respectively. The high removal performance was attributed to negative charges on the membrane surface, branches of dendrimers, and smaller pore size (Fig. 8) [74].

4.4. Recovery of precious metals

Precious metals play a crucial role in biomedicine, agriculture, catalysis, electrical and high-tech industries due to their specific chemical (catalytic activity, corrosion resistance) and physical properties (electrical conductivity) [75–77]. Because of their limited availability and economic relevance, their recovery is economically attractive [78]. Precious metal reserves are scarce and recovery is the only option to meet the growing demand. In 2019, nearly 1100 tons of Ag (17% of the consumption), 130 tons of Au (87% of the consumption), and 49 tons of Pt-group metals (Pt, Pd, Ir, Os, Rh, Ru) were produced by recycling processes in the United States as per U.S. Geological Survey, 2020. Dendrimers-based adsorbents are suitable for the recovery of precious metals. Their well-defined molecular composition with N-bearing functionalities lead to selective extraction of metal ions from aqueous, non-aqueous solutions, and seawater [79–82].

Zhang and coworkers evaluated Au(III) recovery employing silica-gel-based adsorbents modified with PAMAM dendrons (SG-DETA and SG-DETA2). The maximum capacity of 411.7 and 417.6 mg g^{-1} was observed for SG-DETA and SG-DETA2, respectively, with high selectivity in binary metal solutions. The adsorption mechanism of Au(III) onto on SG-DETA and SG-DETA2 involved the exchange of protons bonded to the amine sites with

Au(III) ions and electrostatic interaction in acidic conditions (Fig. 9A) [83].

Zhang et al. carried out experimental and DFT studies to propose a possible mechanism for the adsorption of Ag(I) onto sulfur-capped PAMAM dendrimers-functionalized silica (SG-MITC-G0 ~ SG-MITC-G2.0). The Ag(I) adsorption capacity followed the trend as SG-MITC-G2.0 > SG-MITC-G1.0 > SG-MITC-G0. Since a high generation sulfur-capped PAMAM dendrimer possess more functional groups, adsorption capacity increased with the increase in dendrimer generation. SG-MITC-G0 ~ SG-MITC-G2.0 exhibited excellent adsorption selectivity for Ag(I) in the presence of Zn(II), Fe (II), and Cd(II). Based on the DFT calculations, Ag(I) interacted with one sulfur atom of G0-MITC. The Ag(I) ions interacted with G1.0-MITC via a sulfur atom, carbonyl oxygen atom, and tertiary amine group to form bi-, tri-, tetra-, and penta-dentate complexes. Also, charge transfer from G0-MITC and G1.0-MITC to Ag(I) was predicted during the coordination (Fig. 9B) [84]. Luan et al. immobilized sulfur-functionalized PAMAM dendrimer on magnetic Fe$_3$O$_4$@SiO$_2$ composite for efficient and selective sequestration of Ag (I). Maximum uptake of 139.3 mg g^{-1} was observed for Ag(I) (soft Lewis acid) using the 2nd generation of sulfur functionalized PAMAM due to the introduction of sulfur groups (soft Lewis base) on the periphery of the dendrimer. The adsorption mechanism involved the interaction of sulfur, carbonyl oxygen, and tertiary amine nitrogen groups of sulfur-functionalized PAMAM dendrimer with the Ag(I) ions [82].

Yen et al. reported the fabrication of G3 PAMAM-modified magnetic nanoparticles (MNP-G3) for Pd(IV), Au(III), Pd(II), and Ag(I) recovery from aqueous solutions. MNP-G3 showed a higher adsorption capacity for tri- and tetravalent ions (Pd(IV) and Au (III)). A maximum adsorption capacity of 3.6, 3.6, 2.6, and 2.8 mg g^{-1} was reported for Pd(IV), Au(III), Pd(II), and Ag(I), respectively. It was estimated that Pd(IV) and Au(III) recovery process involved complexation reactions and electrostatic interactions [79].

4.5. Recovery of f-metals

The increasing energy demand has made nuclear energy as an alternative energy source. The mining industry, fuel fabrication and processing, research laboratories, radioisotopes production for nuclear medicine, and military industry are major sources of nuclear waste. The existence of radionuclides with several fission products of neptunium (^{237}Np), plutonium (^{239}Pu), americium ($^{241/243}$Am), and curium (^{245}Cm) in nuclear waste is a threat to human health and the environment [85]. Uranium is used as a fuel in nuclear power plants, in nuclear weapon production, in the electron microscope, and as catalysts in industrial processes. These anthropogenic activities produce a large volume of highly toxic and radioactive waste. Human exposure to a low dosage of uranium can affect the functioning of the liver, heart, and kidneys. Moreover, radionuclides classified as α-emitters (^{239}Pu, ^{237}Np, $^{241/243}$Am, and ^{245}Cm) and β-emitters (^{99}Tc and ^{129}I) are considered as the most dangerous elements to human health and the environment due to their long half-lives. Along with relatively long half-lives, their high mobility in an aqueous environment allows them to be incorporated in the food chain.

Rare earth elements (REEs) are used in various technological devices, including electric cars, smartphones, wind turbines, superconductors, and magnets [86,87]. The consumption of rare earth metal has increased with the development of world economics. REEs are emerging contaminants, which has significant monetary value if recovered from the polluted sources Also, it is known that rare earth metals exhibit hepatotoxic and neurotoxic effects. REEs have been traced in human hair, nails, and biofluids. In humans, REEs cause nephrogenic systemic fibrosis and severe damage to nephrological systems, dysfunctional neurological disorder,
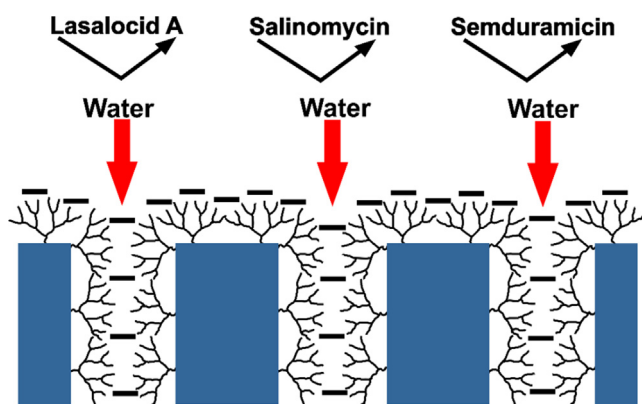

Fig. 8. PAMAM-coated membranes for removing veterinary antibiotics [74].
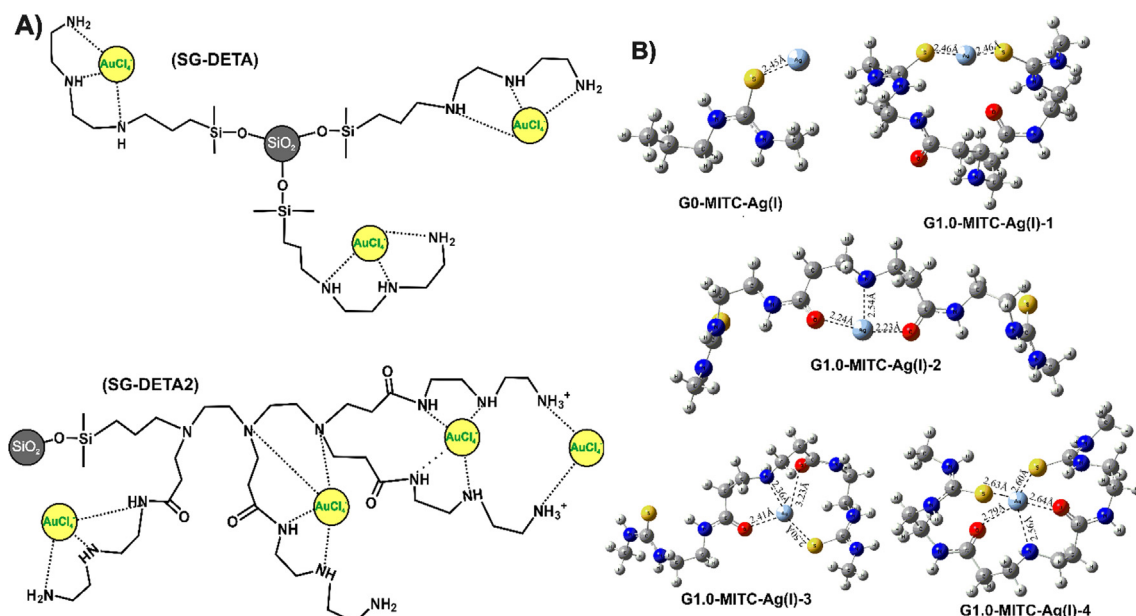
Fig. 9. (**A**) Possible bonding mode of SG-DETA and SG-DETA2 on silica gel surface with favourable bindings of Au(III) with the amino group [83]; (**B**) Optimized geometries for Ag(I) complexation with G0-MITC and G1.0-MITC [84] (Reproduced with permission from Elsevier 2021).

fibrotic tissue injury, oxidative stress, pneumoconiosis, cytotoxicity, anti-testicular effects, and male sterility [86,88,89].

Considering the toxicity and economic value of radionuclides and rare earth elements, their removal and recovery from nuclear wastes and contaminated water bodies have been prioritized. For this, the design of selective, efficient, and low-cost materials for radionuclides recovery is required [90,91]. Recently, dendrimer-based materials have gained attention to produce robust adsorbent with exceptionally high sequestration capacities. Among them, PAMAM is one of the most used dendrimers for the preparation of adsorbents for f-cation recovery.

The properties of multi-walled CNTs (MWCNTs) such as acid, radiation, and chemical stability along with a high sorption capacity, make them an interesting candidate for diverse applications. The functionalization of MWCNT has been a topic of interest for its application in the separation of metal ions. Kumar *et al.* reported PAMAM-functionalized CNTs as novel adsorbents for Pu(IV) removal [92]. G1 and G2 PAMAM dendrimers grafted MWCNT (MWCNT-PAMAMG1 and MWCNT-PAMAMG2) were found efficient in selective removal of Pu(IV) with the highest sorption capacity of 92.5 mg g^{-1} for MWCNT-PAMAMG2. At pH < 4, the amine groups were protonated and the amide carbonyl groups were available for coordination with the Pu(IV) ions. The same materials were employed by Sengupta and co-workers for studying Np removal from nuclear waste solutions [93]. The study reported high radiolytic stability of MWCNT–PAMAM sorbents where the sorption performance decreased slightly for irradiated sorbents, which make these adsorbents suitable for nuclear waste management. In a similar study on the sequestration of Am(III), MWCNT-PAMAMG1 and MWCNT-PAMAMG2 irradiated with a 500 kGy of gamma dose showed an insignificant loss in the Am (III) uptake capacity. The highest adsorption capacity of 97.6 mg g^{-1} was recorded for MWCNT-PAMAMG2 where amidoamine groups showed strong chemical coordination with Am^{3+} ions [94].

Shaaban *et al.* proposed PAMAM-modified silica gel (Si-6G PAMAM) adsorbent for U(VI) capture. Si-6G PAMAM was used for U(VI) adsorption in batch and fixed-bed column configurations. The highest adsorption capacity of 303.0 mg g^{-1} was observed in batch studies. Whereas, in column studies, it was 201.8 mg g^{-1} at a bed height of 1 cm and a flow rate of 1 mL min^{-1} [95]. With

a similar goal of uranium extraction, a new hyperbranched PAMAM-modified adsorbent (PAO-h-PAMAM) was proposed by grafting h-PAMAM onto polyacrylonitrile fibres. The PAOh-PAMAM adsorbent showed a maximum adsorption capacity of 441.0 mg g^{-1} for uranium extraction from seawater. Also, PAO-h-PAMAM exhibited excellent antibacterial activity against marine bacteria and retained its sequestration property for multiple adsorption-desorption cycles. From XPS results it was evident that the amino and amidoxime groups chelated U(VI) during the adsorption process and the synergistic effect between amino groups and amidoxime groups improved the adsorption performance [96].

Priyadarshini *et al.* studied the recovery of U(VI) and Th(IV) from nuclear waste solutions using novel adsorbents fabricated by grafting PAMAM- and diglycolamic acid (DGA)-functionalized PAMAM dendrons over styrene-divinylbenzene solid support (PAMAM–SDB and DGA–PAMAM–SDB). PAMAM–SDB chelating resin was selective towards U(IV) and Th(IV) in the presence of other cations. The principal species involved in the U(VI) adsorption mechanism were the dimeric $[(UO_2)_2(OH)_2]^{2+}$ and trimeric $[(UO_2)_3(OH)_5]^+$ ions at pH 5.5, which interacted with the neutral (in PAMAM–SDB) and negatively charged (in DGA–PAMAM–SDB) functionalities. A higher Th(IV) adsorption capacity was due to the higher ionic potential of hydrolyzed Th(IV) species, which interacted strongly with the neutral and negatively charged resin [97].

Pahan and co-workers reported a PAMAM-functionalized chitosan biopolymer (CTS-N) for the separation of trivalent f-cations. The G3 PAMAM-functionalized chitosan (CTS-3.0) showed quantitative removal of Am(III) and Eu(III) from acidic aqueous medium. Primary, secondary, and tertiary amines along with O-bearing functionalities in CTS 1.0, 2.0, and 3.0 served as complexing sites for Am(III) and Eu(III) ions (Fig. 10A). The adsorbent showed a high degree of reusability up to 10 adsorption-regeneration cycles [98]. PAMAM-immobilized mesoporous silica foam (PAMAM@GTA-NH$_2$-MSF) and fibrous nano-silica KCC-1 (PAMAM@GTA-NH$_2$-KCC-1) were reported for the removal and recovery of trivalent f-cations from waste solutions. The maximum Am(III) uptake capacity of 132.4 and 88.7 mg g^{-1} was recorded for PAMAM@GTA-NH$_2$-MSF and PAMAM@GTA-NH$_2$-KCC-1, respectively. The adsorption of REEs followed the order: Gd^{3+} > Nd^{3+} >
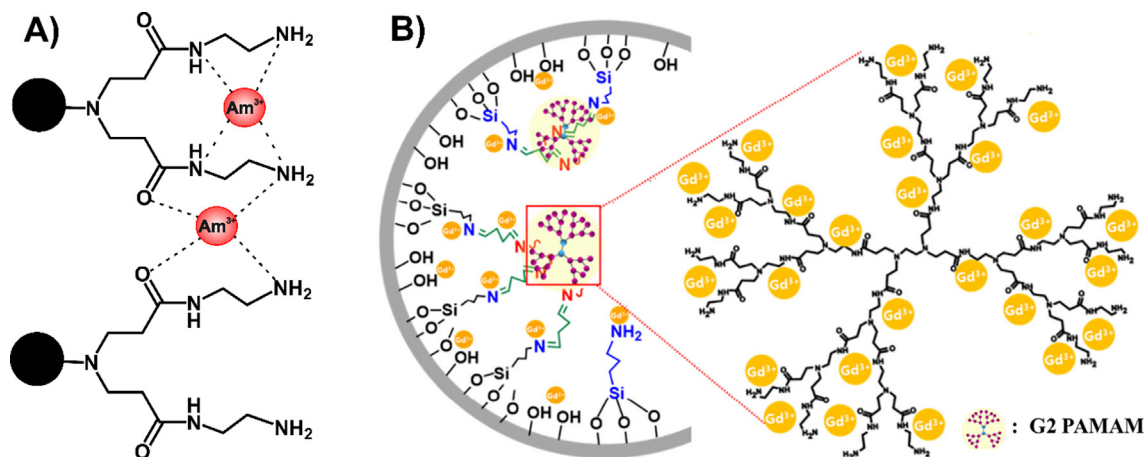
Fig. 10. (**A**) Possible adsorption mechanism of Am^{3+} over CTS-1.0 [98]; (**B**) Proposed adsorption sites for Gd^{3+} in PAMAM@GTA-NH$_2$-MSF [99] (Reproduced with permission from Elsevier 2021).

Ce^{3+} > La^{3+} for both adsorbents, which was in accordance with the order of the ionic radii, La^{3+} (1.03 Å) > Ce^{3+} (1.02 Å) > Nd^{3+} (0.98 Å) > Gd^{3+} (0.93 Å). A cation with a smaller ionic radius has a higher charge density, which improved its interaction with the electron-donating amine and amide functionalities. Also, the hydroxyl density over the silica support provided additional binding sites for the trivalent f-cations (Fig. 10**B**) [99].

4.6. CO$_2$ capture and conversion

The rapid industrialization of the world has increased the energy demands to an exceptionally high level. The surging energy requirements are being fulfilled by burning conventional fossil fuels, which has adverse effects on the environment. The release of large volumes of carbon dioxide (CO_2) from the burning of fossil fuels disrupts the global climate cycle. CO_2 is a greenhouse gas, which is blamed for increasing global temperature (global warming) and followed up catastrophic events like elevated sea-level, flooding, extreme weather events, famine, and wildlife habitat destruction [112]. The Paris Agreement 2015 highlighted the need to control and lower the emission of greenhouse gases. The concerned parties agreed to keep the global temperature increase below 2 °C above pre-industrialized levels by the end of this century [113]. To fulfil these challenging goals, simple and affordable technologies are required for CO_2 capture, storage, and utilization. Amine-based chemical absorption processes have gained widespread attention due to low temperature and low CO_2 partial pressure requirements. Aqueous solutions of amine (monoethanolamine, diglycolamine, diethanolamine, diisopropanolamine, triethanolamine, and methyldiethanolamine) have been widely used for CO_2 capture in cement industries, iron and steel manufacturing, and fossil fuel power plants [114]. The reversible chemical reaction of CO_2 with a primary (**Eq. (1)**) or secondary amine (**Eq. (2)**) yields carbamate ions by Zwitterion mechanism. Whereas, CO_2 reaction with tertiary amine generates bicarbonate ions by the base-catalyzed hydration of CO_2 due to the absence of necessary N—H bond (**Eq. (3)**) [115]. These reactions are reversible and the adsorbed CO_2 can be released by heating the CO_2-saturated absorbents.
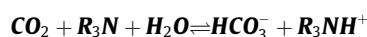
Eq. (1): CO_2 reaction with primary amine:

$$CO_2 + 2RNH_2 \rightleftharpoons RNHCOO^- + RNH_3^+$$

Eq. (2): CO_2 reaction with secondary amine:

$$CO_2 + 2R_2NH \rightleftharpoons R_2NCOO^- + R_2NH_2^+$$

Eq. (3): CO_2 reaction with the tertiary amine in moisture:

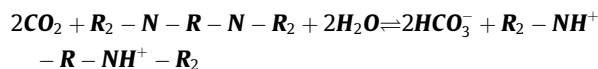$$CO_2 + R_3N + H_2O \rightleftharpoons HCO_3^- + R_3NH^+$$

Just like soluble amines, different generations of PAMAM dendrimers in ionic liquids [116,117], blended with membranes [118–121], and grafted on porous solid materials [122,123] have been extensively explored for CO_2 capture and conversion. A G0 PAMAM dendrimer has four primary amine groups and two tertiary amine groups. In the absence of water, only primary amine groups of the dendrimer molecule react with CO_2 (**Eq. (4)**). Moreover, the CO_2 adsorption/absorption increases significantly in the presence of moisture due to the involvement of tertiary amine groups, along with the primary amine groups (**Eq. (5)**) [116].

Eq. (4): CO_2 reaction with primary amine groups of G0 PAMAM:

$$4CO_2 + 2R(NH_2)_4 \rightleftharpoons R(NHCOO^-)_4 + R(NH_3^+)_4$$

Eq. (5): CO_2 reaction with tertiary amine groups of G0 PAMAM:

$$2CO_2 + R_2 - N - R - N - R_2 + 2H_2O \rightleftharpoons 2HCO_3^- + R_2 - NH^+ - R - NH^+ - R_2$$

An amine-ionic liquid system is a better alternative for the aqueous amine solution as it increases CO_2 absorption rate, reduces amine loss, and decreased energy consumption during the CO_2 stripping [124]. Chau and coworkers have extensively explored PAMAM dendrimers in ionic liquids for CO_2 absorption. CO_2 solubility was studied in 20 wt% G0 PAMAM in 1-butyl-3-me thyl-imidazoliumdicyanamide ([bmim][DCA]) as the ionic liquid. CO_2 solubility in the absorbent system increased with the increasing PAMAM concentration. In the FTIR spectroscopic analysis, the band at 1651 cm^{-1} decreased in intensity while the bands at 1567 and 1170 cm^{-1} increased in intensity after the introduction of CO_2 in the PAMAM-IL system. These changes confirmed that CO_2 reacted with the primary amine groups to yield carbamate ions. Moreover, with the introduction of moisture in the absorbent, CO_2 solubility drastically increased due to the participation of tertiary amine groups of PAMAM [116]. PAMAM-ionic liquid absorbents in hollow fibre membrane contactor have been proposed as a cost-cutting solution for CO_2 capture from post-combustion flue gas (Fig. 11) [117,125]. An 80 wt% G0 PAMAM in [bmim][DCA] was used as the solution to absorb CO_2 from the flue gas. The equilibrium CO_2 concentration in the absorbed reached as high as 6.37 mmol g^{-1} at 50 °C in the presence of moisture. Using the temperature swing method (85–97 °C), absorbed CO_2 was stripped [117] as the increasing temperature lowers the solubility of CO_2
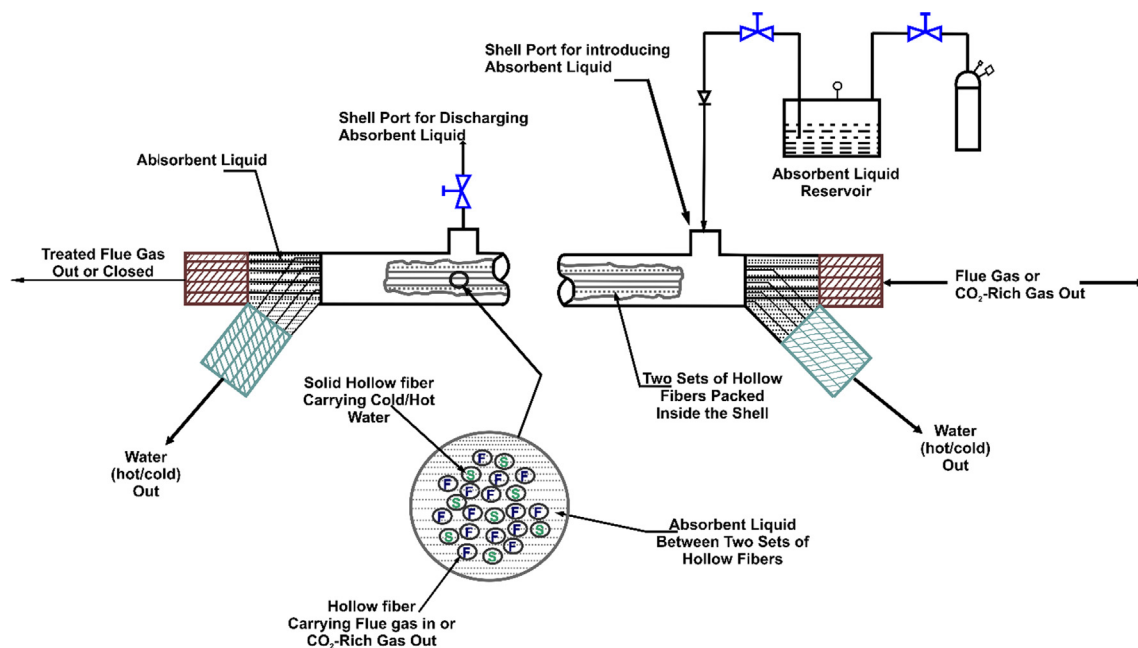
Fig. 11. Schematic of two hollow fibre set-based cylindrical temperature swing membrane absorption device [117].

in PAMAM-IL absorbents [116]. The bands at 1471, 1436, and 1374 cm^{-1} in the FTIR spectrum of CO_2 exposed PAMAM-IL absorbent confirmed bicarbonate formation (**Eq. (5)**) [117].

Ordered mesoporous silica substrates like SBA-15 and MCM-41 are known for their large surface area, uniform porosity, and flexible surface chemistry. An easy surface modification of mesoporous silica substrates with task-specific functionalities has been acknowledged by their diverse environmental applications like wastewater treatment [126] and CO_2 adsorption and separation [127,128]. Moreover, various amine-functionalized silica adsorbents have been studied for selective CO_2 capture [129]. Likewise, reports are available on the use of PAMAM-modified ordered mesoporous silica substrates for CO_2 adsorption. Fadhel *et al.* [130] studied CO_2 adsorption over 50 wt% PAMAM impregnated SBA-15 adsorbents. Out of the four generations of PAMAM dendrimers (G0, G1, G2, and G3) used, G0 showed the highest CO_2 adsorption capacity, which was due to the highest proportion of primary terminal amine groups (9.1 wt% as compared to 5.6 wt% in G3). The study showed that the neat PAMAM dendrimers had a poor CO_2 loading capacity. The molecular dynamic simulations suggested that due to the strong intermolecular hydrogen bonding in neat dendrimers, the CO_2 diffusion was restricted. But, impregnated dendrimers were found to spread over the SBA-15 surface. This spread disrupts the intermolecular hydrogen bonding and improves the CO_2 diffusion process. Miyamoto *et al.* [123] studied the effect of PAMAM loading on CO_2 adsorption characteristics of PAMAM-impregnated MCM-41. The surface area and porosity of impregnated MCM-41 significantly reduced with the increase in PAMAM loading from 0 to 80 wt%. Increasing PAMAM loading favoured the CO_2 adsorption at low CO_2 partial pressure in dry conditions due to an easy formation of carbamate species. But, at high CO_2 partial pressures, the adsorption capacity decreased with increasing PAMAM loading due to a decrease in the surface area and porosity. Thus, for a high CO_2 adsorption capacity, the PAMAM loading should be tuned to avoid excessive loss in the surface area and porosity.

Clay materials are promising adsorbents due to their low cost, easy availability, and natural occurrence. Moreover, these materials could be modified with organic functionalities for the target pollutant. Like amine-modified clays [131,132], PAMAM-modified clays have been reported for selective CO_2 capture [122,133]. Cation-exchange (laponite and sericite) and anion-exchange (hydrotalcite) clays were modified with G4 (amine-terminated PAMAM dendrimer) and G4.5 (carboxylate-terminated PAMAM dendrimer), respectively, for selective CO_2 capture. The pristine clays showed good adsorption capacity in the order of laponite (~11.5 mg g^{-1}) > hydrotalcite (~8.0 mg g^{-1}) > sericite (~3.0 mg g^{-1}) was according to the respective surface area. PAMAM-loaded cationic clays showed a completely different behaviour than the anionic clay. For the cationic clays, increasing cationic dendrimer loading favoured the CO_2 adsorption process. Whereas, for the anionic clay, increasing anionic dendrimer loading lowered the CO_2 adsorption capacity. These two different mechanisms were due to the differences in the CO_2 interaction with G4 and G4.5 dendrimers. G4 with terminal amine groups has a strong affinity for CO_2, whereas, G4.5 with terminal carboxylate groups interacts poorly with CO_2 molecules. Moreover, the loading of PAMAM dendrimers lowered the surface area and was the main reason behind the poor performance of anionic clay. The CO_2 desorption at 40 °C from the pristine clay was better than the organoclays, which suggested CO_2 physisorption over clay and chemisorption on PAMAM dendrimer [122]. Further clarification on different adsorption behaviour was explored by adsorbing NH_3 gas (basic gas) over the organoclays. For NH_3 adsorption, reverse trend as that of CO_2 (acidic gas) was observed. Thus, cationic and anionic organoclays have intrinsic selective uptake for CO_2 and NH_3, respectively [133]. The CO_2 interaction with organoclay was studied by solid-state nuclear magnetic resonance (NMR) spectroscopy with isotope-enriched $^{13}CO_2$. The ^{13}C NMR spectrum of CO_2-adsorbed pristine laponite had two signals with ^{13}C chemical shift (δ) of 162 and 167 ppm for carbon in the bicarbonate and carbonate, respectively. These species formed after reaction with sodium silicate in laponite with adsorbed CO_2 in the presence of water. On the contrary, for CO_2-adsorbed laponite, a strong signal at δ = 164 ppm and a very weak signal at δ = 162 ppm was observed. The signal at 164 ppm confirmed the formation of carbamate species. These observations strongly suggested that in the organoclays, a large proportion of CO_2 was captured by the terminal groups of PAMAM [133].

PAMAM-hydrotalcite could be blended with carboxymethyl chitosan (CMC) to fabricate a thermally stable membrane for selective CO_2 separation. The interlayer hydrated carbonate anions in Mg-Al-carbonate hydrotalcite serve as the carrier for easy CO_2 transportation by forming bicarbonates after reacting with CO_2. Moreover, Mg^{2+} and Al^{3+} cations act as the CO_2 adsorption sites. The choice of CMC as the membrane matrix was due to its exceptional CO_2 permeance and possible hydrogen bonding between the amide groups of CMC and the hydroxyl groups of hydrotalcite. The fabricated membrane had high CO_2 permeance (76 GPU) where the CO_2/N_2 selectivity reached 312 at 90 °C [120]. Poly(vinyl alcohol) (PVA) with a cross-linking agent (organic titanium compounds) is a well-researched membrane matrix for the fabrication of PAMAM-based membranes [118,134–136]. These PAMAM/cross-linked PVA membranes have been extensively studied for the selective separation of moist CO_2 with a detailed investigation on the experimental parameters like CO_2 partial pressure, temperature, membrane thickness, and type and concentration of crosslinkers.

Though these parameters are important for determining the maximum CO_2 permeance and selectivity, we are focused on the parameters like the effect of PAMAM concentration and the presence of amine additives like amino acids. Duan *et al.* 2012 [134] studied the effect of PAMAM concentration on the CO_2 separation properties of PAMAM/cross-linked PVA membrane at low and high CO_2 partial pressure. With the increasing PAMAM concentration, the CO_2 permeance increased continuously at low pressure. Whereas, at high pressure, the CO_2 permeance increased, which was followed by a sharp dip at the highest PAMAM loading of 82.8 wt% dendrimer fraction. A high PAMAM concentration assures high CO_2 solubility due to the presence of a large number of primary amino groups. But, the decrease at a high CO_2 partial pressure could be due to the low-pressure tolerance of the membrane containing a higher PAMAM proportion. Amino acids are suitable additives to improve the CO_2 separation performance due to the presence of amine groups. Thus, amino acids as additives could enhance CO_2 permeance and selectivity. Duan *et al.* 2013 [135] reported proline as a better additive for achieving higher CO_2 permeance and selectivity than glycine or 2,3-diaminopropionic acid. Proline with an N-heterocyclic ring has a crowded amino group as compared to glycine and 2,3-diaminopropionic acid. The stearic hindrance effect lowers the tendency of the amino group to form carbamate ions, which increases CO_2 uptake [137]. Taniguchi *et al.* 2008 [138] studied the effect of different generations of PAMAM dendrimer on CO_2 separation properties by immobilizing PAMAM in a cross-linked poly(ethylene glycol) matrix. Both CO_2 and H_2 permeance increased with the PAMAM generation from G0 to G5, which decreased the CO_2 selectivity. Though the number of primary amines increases with the PAMAM generation, the amine density per unit mass of dendrimer decreases. Moreover, large dendrimer molecules disfavour the cross-linking process, which creates free volume in the polymeric membrane. The formation of the large free volume is responsible for significant permeability of small molecules like H_2. Because of this, most often lower generations of PAMAM (G0 or G1) have been used in the fabrication of PAMAM-based membranes for highly selective separation of CO_2 [138–140].

4.7. Sensors for pollutant detection

The high specific surface area and the large number of functional groups of PAMAM make them suitable candidates to develop sensitive and specific sensors to determine pollutants such as organic molecules and metal ions in solution. Particularly, the large surface area allows the supporting of different receptors selective to the targeted pollutant, and the presence of functional groups

enhance the pollutants uptake. A comprehensive description of the use of PAMAM as amplifiers, receptors, linkers, and transducers for sensing applications has been reported recently [141]. However, in this section, the application of PAMAM and diverse modifications reported in literature dealing with the sensing of organic pollutants and metal ions in the last decade have been elaborated in detail. Table 2 summarizes reported studies on PAMAM-based dendrimers as sensors of pollutants. Early works reported the incorporation of PAMAM in amperometric sensors to enhance the geometric area of the electrode. Recently, the trend is to take advantage of its tunable highly branched structure to immobilize a large number of recognition elements targeted for a specific pollutant and enhance its signal. In this way, very low detection limits have been reported in a wider concentration range.

Algarra *et al.* developed an optical sensor for nitroaromatic compounds using a nanocomposite of PAMAM and CdSe quantum dots (QDs). CdSe QDs were directly grown over the PANAM structure and the improved affinity of the composite was associated with the structural alterations of the QDs. This altered the fluorescence emission response as a consequence of variation on the quantum confinement regiment [142]. A more complex structure was employed by Li *et al.* to obtain an immunosensor for benzo[a]pyrene detection. First, a layer of poly 2-amino-5,2′:5′,2″-terthiophene (PATT) was electrochemically grown on a gold electrode, then PAMAM was drop cast, and finally, enzymes were immobilized on PAMAM's functional groups. The combination of different components in the electrodes enhanced signal response due to the covalent interaction between PATT and PAMAM and high loading of enzymes in PAMAM functionalities, allowing the determination of benzo[a]pyrene at low concentrations [143].

The coupling of carbon structures with PAMAM nanocomposites is a successful strategy to develop amperometry sensors. Qu *et al* employed G4 PAMAM-NH_2 modified with Au as a linker to retain the acetylcholinesterase enzyme and sense carbofuran pesticide in water. The electrode consisted of a film of CNTs to provide high conductivity and a layer of PAMAM-Au composite to retain the enzyme. The multilayered film developed exhibited a linear variation of current with the carbofuran concentration in the range of 4.8 to 90 nM, with a detection limit of 4.0 nM [144]. Yin *et al.* employed the drop-casting technique to modify a Fe_3O_4/glassy carbon electrode with PAMAM and improve its sensing ability for the determination of bisphenol A in milk samples [145]. The same research group also developed a sensor for determining bisphenol A in water by combining CdTe QDs and G4 PAMAM [146]. While Fe_3O_4 or CdTe offered an electrocatalytic substrate to irreversibly oxidize bisphenol A, PAMAM with easily protonable amino groups enhanced the surface accumulation of negatively charged bisphenol A. The synergistic interaction between these components caused an enlargement of registered currents and displacement of current peak potential towards less positive values. However, a larger detection range and a lower detection limit were observed when using CdTe QDs. The ability of the sensor to measure the bisphenol A concentration in real samples was also validated by the authors.

Zhou's research group have recently developed a new methodology by coupling magnetic solid-phase extraction with high-performance liquid chromatography (MSPE-HPLC) for the determination of several organic pollutants (such as phenols, phthalate esters, organochlorine pesticides, and polycyclic aromatic hydrocarbons) in water in trace levels [108,147–149]. For this purpose, Fe_3O_4 nanoparticles were functionalized with different generations of PAMAM to overcome poor selectivity and weak adsorption energy of bared magnetite nanoparticles, but still using its magnetic behaviour for a rapid recuperation of solids from solution. The Fe_3O_4@PAMAM platforms can be used several times and the pre-concentration of the pollutant can be improved by grafting

Table 2

PAMAM-based materials for sensing organic pollutants and metallic ions in solution.

Sensor	Sensing methodology	Analyte	Range	Limit of detection
G4 PAMAM/CdSe QDs [142]	Fluorescence	MNP	$0.1–40$ mg L^{-1}	0.1 mg L^{-1}
		ACNB	$0.01–5$ mg L^{-1}	0.01 mg L^{-1}
		MNB	$0.01–0.5$ mg L^{-1}	0.01 mg L^{-1}
PATT/G2 PAMAM-enzymes [143]	Electrochemistry	BaP	$0.01–2.0$ ng L^{-1}	6 pg L^{-1}
CNT/G4 PAMAM-Au [144]	Electrochemistry	Carbofuran	$4.8 \times 10^{-9}–0.9 \times 10^{-7}$ M	4.0×10^{-9} M
Fe$_3$O$_4$/G4 PAMAM [146]	Electrochemistry	BPA	$1.3 \times 10^{-8}–9.9 \times 10^{-6}$ M	1.0×10^{-9} M
CdTe QDs/G4 PAMAM [145]	Electrochemistry	BPA	$1.0 \times 10^{-8}–3.1 \times 10^{-6}$ M	5.0×10^{-9} M
Fe$_3$O$_4$@G1.5 PAMAM [147]	MSPE-HPLC	4-NoP	$0.1–500$ µg L^{-1}	17.0 ng L^{-1}
		TBBPA		11.0 ng L^{-1}
Fe$_3$O$_4$@G1.5 PAMAM [148]	MSPE-HPLC	DPhP	$0.1–600$ µg L^{-1}	25.0 ng L^{-1}
		DCHP	$0.5–600$ µg L^{-1}	11.0 ng L^{-1}
		DnPP	$1–600$ µg L^{-1}	16.0 ng L^{-1}
Fe$_3$O$_4$@G2 PAMAM [108]	MSPE-HPLC	p,p′-DDT	$0.1–500$ µg L^{-1}	12.0 ng L^{-1}
		o,p′-DDT		29.0 ng L^{-1}
		p,p′-DDE		12.0 ng L^{-1}
		p,p′-DDD		16.0 ng L^{-1}
Fe$_3$O$_4$@G3 PAMAM@4-MBA [149]	MSPE-HPLC	PHE	$0.1–300$ µg L^{-1}	14.0 ng L^{-1}
		Ant		32.0 ng L^{-1}
		FLT		50.0 ng L^{-1}
		PYR		27.0 ng L^{-1}
		BaP		39.0 ng L^{-1}
Fe$_3$O$_4$@G2 PAMAM [150]	MSPE-HPLC	Cd^{2+}	$4.4 \times 10^{-10}–1.8 \times 10^{-6}$ M	1.4×10^{-10} M
		Hg^{2+}	$5.0 \times 10^{-9}–1.0 \times 10^{-5}$ M	5.0×10^{-10} M
TREN/G4 PAMAM/Ag [151]	Colorimetry	Hg^{2+}	$8.5 \times 10^{-8}–4.7 \times 10^{-6}$ M	5.9×10^{-9} M
SWCNT/G4 PAMAM/enzymes [152]	Electro-chemiluminescence	Hg^{2+}	$7.0 \times 10^{-12}–5.0 \times 10^{-8}$ M	2.4×10^{-12} M
Fe$_3$O$_4$@SiO$_2$/G4 PAMAM/QDs [153]	Electro-chemiluminescence	Hg^{2+}	$2.0 \times 10^{-17}–2.0 \times 10^{-6}$ M	2×10^{-18} M
G1 PAMAM/4-methylpiperazine-1,8-naphthalimide [154]	Fluorescence	Sn^{2+}	$0–2.7 \times 10^{-4}$ M	3.3×10^{-6} M
G1 PAMAM/4-N,N-dimethylaminoethyloxy-1,8-naphthalimide [156]	Fluorescence	Cu^{2+}	$0–1.0 \times 10^{-5}$ M	1.4×10^{-6} M
G1 PAMAM/4-amino-1,8-naphthalimide [157]	Fluorescence	Ag$^+$	$0.3 \times 10^{-4}–4.8 \times 10^{-4}$ M	–
G0 PAMAM/Curcumin [158]	Fluorescence	Cu^{2+}	$0–3.6 \times 10^{-5}$ M	–
Carbon QDs@G4 PAMAM [159]	Fluorescence	[PtCl$_6$]$^{2-}$	$6.0 \times 10^{-6}–9.6 \times 10^{-5}$ M	6.6×10^{-7} M
Porphyrin@G2.5 PAMAM [160]	Fluorescence	Li$^+$	$0.1 \times 10^{-6}–5.0 \times 10^{-6}$ M	1.3×10^{-8} M

MNP: 4-methoxy-2-nitrophenol; ACNB: 2-amine-5-chloro-1,3-dinitrobenzene; MNB: 3-methoxy-4-nitrobenzoic acid; 4-NoP: 4-nonylphenol; TBBPA: tetrabromobisphenol A; DPhP: dibenzyl phthalate; DnPP: dibutyl phthalate; DCHP: dicyclohexyl phthalate; DDT: dichlorodiphenyltrichloroethane; DDE: dichlorodiphenyldichloroethylene; DDD: dichlorodiphenyldichloroethane; PHE: phenanthrene; ANT: anthracene; FLT: fluoranthene; PYR: pyrene; BaP: benzo(a)pyrene.

4-mercaptobenzoic acid. Finally, the pollutant is extracted using a proper eluent to determine its concentration using HPLC. This new methodology reduces the consumption of solvents and analytical time compared to traditional liquid-liquid extraction [149]. The MSPE-HPLC analysis method has been employed for the simultaneous determination of trace levels Cd^{2+} and Hg^{2+} ions using a Fe$_3$O$_4$@PAMAM composite. However, interference of other metal cations such as Zn^{2+}, Ni^{2+}, and Cu^{2+} is expected due to competitive adsorption [150].

Gürbürz *et al.* designed a colourimetric sensor for Hg^{2+} ions. The composite consisted of a core of Tris(2-aminoethyl)amine (TREM) modified with PAMAM obtained by microwave synthesis. Then, Ag nanoparticles were formed directly on the composite through chemical reduction of Ag$^+$ with NaBH$_4$. The variation in the intensity of the Ag plasmonic signal together with a blue shift in the wavelength was sensitive to the concentration of Hg^{2+} in solution since an Ag-Hg amalgam formed *in-situ* during the measurement. The yellow colour of the suspension of the TREM/PAMAM/Ag composite in solution did not change in presence of other metal ions, showing this method is specific to Hg^{2+} [151]. Ma *et al.* designed a sensor for selectively determining Hg^{2+} in solution by tethering an Hg^{2+} specific oligonucleotide to a PAMAM dendrimer. The complexation reaction between Hg^{2+} and thymine bases resulted in a measurable increment in the electro-chemiluminescence. The selectivity of the electrode towards Hg^{2+} ions was tested in presence of several divalent metal ions and inorganic cations. Additionally, the electrode was regenerable and satisfactorily measured Hg^{2+} in real samples [152]. Fe$_3$O$_4$@SiO$_2$/PAMAM/QDs electrode was reported for ultrasensitive determination of Hg^{2+} through electro-chemiluminescence. This new approach enhanced in various order of magnitude the range for sensing the Hg^{2+} with a very

low detection limit. The greatly amplified electro-chemiluminescence signal was observed due to the complex nano-architecture designed in this work. Additionally, the formed electrode showed satisfactory results for measuring the Hg^{2+} in a fish sample and tap water [153].

Another attractive approach to measured metal ions in solution was reported by Grabchev's group [154,155]. Fluorescent dendrimers were obtained by attaching naphthalimide fluorophores in the periphery of PAMAM. The coordination of the metal ions through the nitrogen atoms with unpaired electrons in the fluorophores alters the fluorescence emitted by the complex. Depending on the dendrimer structures, Li$^+$, Zn^{2+}, Sn^{2+}, Cu^{2+}, and Fe^{3+} ions could be detected. Later, the same research group modified G1 PAMAM with eight 4-N,N-dimethylaminoethyloxy-1,8-naphthalimide units to create a blue fluorescent dendrimer. Although the fluorescence emission of the obtained dendrimer varies with the presence of different metal ions, the best results (lower detection limit and broad concentration range) were obtained for Cu^{2+} ions [156].

Following the same strategy, Dodangeh *et al.* reported the synthesis of 1,8-naphthalimide conjugated PAMAM dendrimer. This material showed high selectivity for sensing Ag$^+$ in a concentration range of $0.3–4.8 \times 10^{-4}$ M but with no linear dependency between fluorescence intensity and Ag$^+$ concentration [157]. Recently, curcumin immobilization on PAMAM dendrimers for sensing metal ions in solution was reported. The fluorescence response of this new dendrimer was quenched in presence of Cu^{2+} with no interference from other metal cations. However, the signal quenching sensitivity to Cu^{2+} ions decreased with the increasing PAMAM generation with the best result observed for G0 PAMAM. The quenching of the fluorescence signal was presumably caused by

the coordination of Cu^{2+} ions to the carbonyl groups of curcumin molecules [158].

A fluorescent sensor for chloroplatinate ions was constructed by coating carbon QDs with PAMAM dendrimer through hydrothermal treatment. Positively charged PAMAM, which is due to the deprotonation of amino groups, is expected to enhance the interaction of $[PtCl_6]^{2-}$ with carbon QDs that are appropriate sensor platforms for easily reducible species. Although some interference was detected in presence of Fe^{3+} and Hg^{2+}, the dendrimer exhibited a high affinity for $[PtCl_6]^{2-}$ ions. The composite exhibited a large concentration range for determining Hg^{2+} (eleven orders of magnitude) with an extremely low detection limit (2×10^{-18} M) [159]. Militello *et al.* reported the performance of a porphyrin modified with PAMAM dendrimer as a candidate to sense Li^+ ions. Variation in the fluorescence response was measured at lithium concentrations considerably lower than those of K^+ and Na^+. The coordination of Li^+ to the four nitrogen atoms at the centre of the porphyrin was favoured by its lower size, forming a square-planar configuration. The more extended linear response to the Li^+ concentration was reached with porphyrin-G2.5 PAMAM [160].

5. Environmental impact of PAMAM

The literature dealing with the environmental applications of dendrimer-based nanomaterials is expanding every year. However, most studies lack systematic investigation of environmental risks associated with the use of dendrimers. Some research works have shown evidence of potential environmental and human hazards of dendrimers in different ecosystems [161,162]. The impact of nanomaterials on the environment requires detail study on their mobility, reactivity, toxicity, and bio-persistence in the environment [163]. In this section, we have discussed the ecotoxicity of PAMAM dendritic nanoparticles on animals, plants, and human beings.

Generally, the chemical composition and dimension of the nanomaterial determine its toxicity. In the case of PAMAM dendrimers, surface charge (nature of terminal groups) and size (generation) mainly regulate the toxicity [164–166]. Researchers have correlated the chemical composition at the surface of PAMAM dendrimer with its toxic response using *in vivo* and *in vitro* models [167,168]. The surface interaction of positively charged dendrimer with the negatively charged biological membranes leads to membrane thinning, nanohole formation, and erosion, which disrupts its biological functioning [162,169]. The studies by Gonzalo *et al.* [170] and Petit *et al.* [171] ratified the toxicity of cationic dendrimers in aquatic microorganisms of environmental significance such as cyanobacterium of the genus Anabaena and the green alga *Chlamydomonas reinhardtii*. Also, Malik *et al.* [172] demonstrated that negatively charged dendrimers are less toxic than the positively charged ones by comparing cytotoxicity of PAMAM with carboxylate, malonate, and amine terminals in cell lines. Similar results were reported by Bodewein *et al.* [173] where anionic G3.5 and G4.5 PAMAM did not show toxicity in zebrafish embryos. On the contrary, cationic PAMAM triggered morphological effects in zebrafish embryos over time (Table 3).

The dose (concentration) is another factor that governs the toxicity of PAMAM dendrimers. This factor is directly proportional to PAMAM generation, indicating that the use of a higher generation and dose of dendritic structures is less environmental benign [174]. *In vitro* mammalian toxicological studies suggest the dependence between the cytotoxic effect and dose/generation of PAMAM dendrimers (G4, G5, and G6) [175,176], and induce apoptosis mediated by mitochondrial dysfunction [177]. Naha *et al.* [178]

Table 3

EC50-values for morphological effects of cationic and anionic dendrimers in zebrafish embryos after exposure at 24 h and 48 h post-fertilization (hpf), including the 95% confidence intervals (95% CI). The values were derived from the concentration-effect correlations using probit analysis (n.d. = non-determinable) [173].

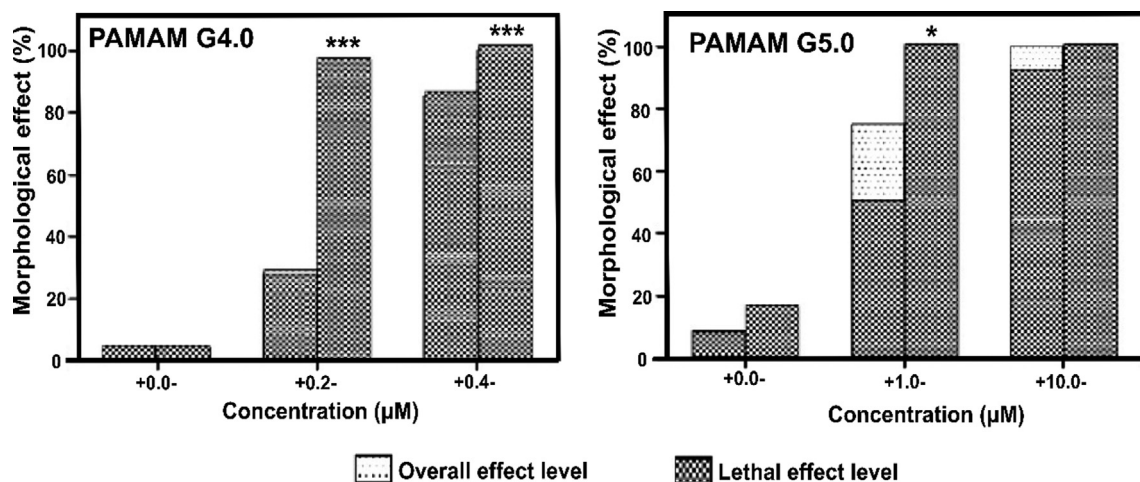| Type	Dendrimer	Number of terminal groups	Zebrafish (24 hpf)		Zebrafish (48 hpf)	
			EC50 [µM]	95% CI [µM]	EC50 [µM]	95% CI [µM]
Cationic	G3.0 PAMAM	32	0.370	0.324–0.417	0.22	0.057–0.397
	G4.0 PAMAM	64	0.221	0.094–0.31	0.161	0.116–0.203
	G5.0 PAMAM	128	1.645	0.911–3.619	0.560	0.189–1.320
Anionic	G3.5 PAMAM	64	n.d	n.d	n.d	n.d
	G4.5 PAMAM	128	n.d	n.d	n.d	n.d

Fig. 12. Effect on apoptosis caused by PAMAMG4.0 (left), G5.0 (right) exposure at 48 hpf. 0.0 represents ISO-water control. The bars depict the mean total number of apoptotic particles counted (±standard error). Stars indicate the level of significance ($*P < 0.05$, $**P < 0.01$, $***P < 0.001$) of the difference in the amount of apoptotic particles between the respective treatment and the control. Significance was determined with a two-sided Student's *t*-test. Diagrams were generated with GraphPad (Version 5.0) [173]. (Modified with permission from Elsevier 2021).

observed that cytotoxicity and toxicity in mouse macrophage cells are dependent on the dose and generation of PAMAM dendrimers (G4, G5, and G6) i.e., the number of anime surface group per generation. Bodewein *et al.* [173] studied the *in vivo* toxicity and cytotoxicity of cationic G3, G4, and G5 PAMAM dendrimers in zebrafish embryos and cancer cells, respectively. The results showed an increase of toxicity over time with EC50 values ranging from 0.16 to 1.7 μM at 24 and 48 hpf, respectively (Table 3). Apoptosis in the embryos raised linearly with PAMAM concentration (Fig. 12). Also, an increase in generation causes higher toxic effects in the HepG2 and DU145 cell lines, but in embryos, it was the opposite. Durocher and Girard [179] reported pro-inflammatory activities as well as the production of several cytokines/chemokines by PAMAM dendrimer in murine air pouch model, which were correlated with dendrimer generation in the order G3 > G2 > G0. In human beings (human skin and intestinal cell models), PAMAM toxicity has been studied by colourimetric assays [180]. The study has proved toxicity reliance on the dendrimer generations and exposure dose.

The application of PAMAM-based materials in wastewater treatment should be supported by an evaluation of their ecotoxicity on living systems. The toxicity is mainly associated with the number of surface amine groups and generation. Developing biocompatible PAMAM dendrimer through surface modification could be an alternative approach to reduce its environmental impact. Surface modification of PAMAM with polyethylene glycol or fatty acids have proven to reduce their toxicity and improve biocompatibility [164]. Also, Kim and Park suggested the use of magnetic-cored dendrimer for an easy and efficient recovery of adsorbent from the aqueous medium [181]. The use of lower PAMAM generations in environmental applications could reduce the environmental impact and improve the efficacy, which has been observed for G0 PAMAM in CO_2 capture and conversion process.

6. Conclusion

The review provides a comprehensive overview of the most relevant topics related to the use of PAMAM-based materials as adsorbents for wastewater treatment. Owing to a three-dimensional dendritic architecture, large internal cavities, and easy surface functionalization, PAMAM dendrimers exhibit excellent adsorptive properties toward a large class of pollutants. However, its recovery from the solution phase represents a challenge for its reusability. The immobilization of dendrimer stands out as an appealing alternative to solve this issue. Among the most used supports for the anchoring of PAMAM are magnetic nanoparticles, carbonaceous, and silica materials. The immobilization of the dendrimer onto said supports can be carried out mainly by two conventional approaches: (a) grafting, which involves the junction of the PAMAM and the support by using a coupling agent and (b) growing, where the dendrimer is grown over the surface of the support. An overview of both immobilization approaches is provided in this review. PAMAM-based adsorbents are suitable for the removal of cationic and anionic organic and inorganic pollutants from wastewater via one of more interactions including electrostatic interactions, hydrogen bonding, and complexation. PAMAM-based materials have been also used as sensors for detection and quantification of different pollutants, mostly metal ions and some organic contaminants. Moreover, the bulk availability of amine groups on the periphery of PAMAM dendrimers makes them excellent absorbent/adsorbent for CO_2 capture and conversion to carbamate or carbonate ions. The review has put great emphasis on the environmental impact of PAMAM use in wastewater treatment. Regardless of the high efficiency of the PAMAM-based materials for water remediation, environmental considerations and cost-benefit analysis are needed in the future reports to evaluate their large-scale application. Nevertheless, large adsorption capacities, tunable surface allowing to deal with a majority of pollutants, and easy preparation and modification, make PAMAM-based adsorbents as promising alternatives for wastewater treatment and carbon capture and conversion technology.

Declaration of Competing Interest

The authors declare that they have no known competing financial interests or personal relationships that could have appeared to influence the work reported in this paper.

References

[1] E. Buhleier, W. Wehner, F. Vögtle, "Cascade"- and "Nonskid-Chain-like" Syntheses of Molecular Cavity Topologies, Synthesis 1978 (1978) 155–158, https://doi.org/10.1055/s-1978-24702.

[2] A. Paolini, L. Leoni, I. Giannicchi, Z. Abbaszadeh, V. D'Oria, F. Mura, A. Dalla Cort, A. Masotti, MicroRNAs delivery into human cells grown on 3D-printed PLA scaffolds coated with a novel fluorescent PAMAM dendrimer for biomedical applications, Sci. Rep. 8 (2018) 13888, https://doi.org/10.1038/s41598-018-32258-9.

[3] A.M.M. El-Betany, E.A. Kamoun, C. James, A. Jangher, G. Aljayyoussi, P. Griffiths, N.B. McKeown, M. Gumbleton, Auto-fluorescent PAMAM-based dendritic molecules and their potential application in pharmaceutical sciences, Int. J. Pharm. 579 (2020), https://doi.org/10.1016/j.ijpharm.2020.119187 119187.

[4] R. Lotfi, B. Hayati, S. Rahimi, A.A. Shekarchi, N.M. Mahmoodi, A. Bagheri, Synthesis and characterization of PAMAM/SiO2 nanohybrid as a new promising adsorbent for pharmaceuticals, Microchem. J. 146 (2019) 1150–1159, https://doi.org/10.1016/j.microc.2019.02.048.

[5] M. Mirzaie, A. Rashidi, H.A. Tayebi, M.E. Yazdanshenas, Optimized Removal of Acid Blue 62 from Textile Waste Water by SBA-15/PAMAM Dendrimer Hybrid Using Response Surface Methodology, J. Polym. Environ. 26 (2018) 1831–1843, https://doi.org/10.1007/s10924-017-1083-5.

[6] F. Vögtle, G. Richardt, N. Werner, Dendrimer Chemistry: Concepts, Syntheses, Properties, Applications, 1st ed., Wiley, 2009. https://doi.org/10.1002/9783527626953.

[7] P.K. Maiti, T. Çaǧin, G. Wang, W.A. Goddard, Structure of PAMAM Dendrimers: Generations 1 through 11, Macromolecules 37 (2004) 6236–6254, https://doi.org/10.1021/ma035629b.

[8] Z. Xu, M. Kahr, K.L. Walker, C.L. Wilkins, J.S. Moore, Phenylacetylene Dendrimers by the Divergent, Convergent, and Double-Stage Convergent Methods, J. Am. Chem. Soc. 116 (1994) 4537–4550, https://doi.org/10.1021/ja00090a002.

[9] D.A. Tomalia, H. Baker, J. Dewald, M. Hall, G. Kallos, S. Martin, J. Roeck, J. Ryder, P. Smith, Dendritic macromolecules: synthesis of starburst dendrimers, Macromolecules 19 (1986) 2466–2468, https://doi.org/10.1021/ma00163a029.

[10] D.A. Tomalia, H. Baker, J. Dewald, M. Hall, G. Kallos, S. Martin, J. Roeck, J. Ryder, P. Smith, A New Class of Polymers: Starburst-Dendritic Macromolecules, Polym. J. 17 (1985) 117–132, https://doi.org/10.1295/polymj.17.117.

[11] H. Fan, X. Ma, S. Zhou, J. Huang, Y. Liu, Y. Liu, Highly efficient removal of heavy metal ions by carboxymethyl cellulose-immobilized Fe3O4 nanoparticles prepared via high-gravity technology, Carbohydr. Polym. 213 (2019) 39–49, https://doi.org/10.1016/j.carbpol.2019.02.067.

[12] B. Ozbey Unal, Z. Bilici, N. Ugur, Z. Isik, E. Harputlu, N. Dizge, K. Ocakoglu, Adsorption and Fenton oxidation of azo dyes by magnetite nanoparticles deposited on a glass substrate, Journal of Water, Process Eng. 32 (2019), https://doi.org/10.1016/j.jwpe.2019.100897 100897.

[13] A. Ghamkhari, L. Mohamadi, S. Kazemzadeh, M.N. Zafar, A. Rahdar, R. Khaksefidi, Synthesis and characterization of poly(styrene-block-acrylic acid) diblock copolymer modified magnetite nanocomposite for efficient removal of penicillin G, Compos. B Eng. 182 (2020), https://doi.org/10.1016/j.compositesb.2019.107643 107643.

[14] H. Park, A. May, L. Portilla, H. Dietrich, F. Münch, T. Rejek, M. Sarcletti, L. Banspach, D. Zahn, M. Halik, Magnetite nanoparticles as efficient materials for removal of glyphosate from water, Nat Sustain. 3 (2020) 129–135, https://doi.org/10.1038/s41893-019-0452-6.

[15] A. Zarei, S. Saedi, F. seidi, Synthesis and Application of Fe3O4@SiO2@Carboxyl-Terminated PAMAM Dendrimer Nanocomposite for Heavy Metal Removal, J. Inorg. Organomet. Polym. 28 (2018) 2835–2843, https://doi.org/10.1007/s10904-018-0948-y.

[16] L. Danyang, N. Lanli, D. Yimin, Z. Jiaqi, C. Tianxiao, Z. Yi, Synthesis of poly (amidoamine) dendrimer-based dithiocarbamate magnetic composite for the adsorption of Co2+ from aqueous solution, J. Mater. Sci.: Mater. Electron. 30 (2019) 1161–1174, https://doi.org/10.1007/s10854-018-0385-2.

[17] M. Ghoochian, H.A. Panahi, S. Sobhanardakani, L. Taghavi, A.H. Hassani, Synthesis and application of Fe3O4/SiO2/thermosensitive/PAMAM-CS nanoparticles as a novel adsorbent for removal of tamoxifen from water samples, Microchem. J. 145 (2019) 1231–1240, https://doi.org/10.1016/j.microc.2018.12.004.

[18] A.A. Tabatabaiee Bafrooee, H. Ahmad Panahi, E. Moniri, M. Miralinaghi, A.H. Hasani, Removal of Hg2+ by carboxyl-terminated hyperbranched poly (amidoamine) dendrimers grafted superparamagnetic nanoparticles as an efficient adsorbent, Environ. Sci. Pollut. Res. 27 (2020) 9547–9567, https://doi.org/10.1007/s11356-019-07377-z.

[19] Y. Zhou, L. Luan, B. Tang, Y. Niu, R. Qu, Y. Liu, W. Xu, Fabrication of Schiff base decorated PAMAM dendrimer/magnetic Fe3O4 for selective removal of aqueous Hg(II), Chem. Eng. J. 398 (2020) 125651, https://doi.org/10.1016/j.cej.2020.125651.

[20] F. Zhang, B. Wang, S. He, R. Man, Preparation of Graphene-Oxide/Polyamidoamine Dendrimers and Their Adsorption Properties toward Some Heavy Metal Ions, J. Chem. Eng. Data 59 (2014) 1719–1726, https://doi.org/10.1021/je500219e.

[21] W. Xiao, B. Yan, H. Zeng, Q. Liu, Dendrimer functionalized graphene oxide for selenium removal, Carbon 105 (2016) 655–664, https://doi.org/10.1016/j.carbon.2016.04.057.

[22] B. Hayati, A. Maleki, F. Najafi, H. Daraei, F. Gharibi, G. McKay, Synthesis and characterization of PAMAM/CNT nanocomposite as a super-capacity adsorbent for heavy metal (Ni2+, Zn2+, As3+, Co2+) removal from wastewater, J. Mol. Liq. 224 (2016) 1032–1040, https://doi.org/10.1016/j.molliq.2016.10.053.

[23] B. Hayati, A. Maleki, F. Najafi, F. Gharibi, G. McKay, V.K. Gupta, S. Harikaranahalli Puttaiah, N. Marzban, Heavy metal adsorption using PAMAM/CNT nanocomposite from aqueous solution in batch and continuous fixed bed systems, Chem. Eng. J. 346 (2018) 258–270, https://doi.org/10.1016/j.cej.2018.03.172.

[24] Y. Niu, R. Qu, H. Chen, L. Mu, X. Liu, T. Wang, Y. Zhang, C. Sun, Synthesis of silica gel supported salicylaldehyde modified PAMAM dendrimers for the effective removal of Hg(II) from aqueous solution, J. Hazard. Mater. 278 (2014) 267–278, https://doi.org/10.1016/j.jhazmat.2014.06.012.

[25] M. Pawlaczyk, G. Schroeder, Efficient Removal of Ni(II) and Co(II) Ions from Aqueous Solutions Using Silica-based Hybrid Materials Functionalized with PAMAM Dendrimers, Solvent Extr. Ion Exch. 38 (2020) 496–521, https://doi.org/10.1080/07366299.2020.1766742.

[26] G. Amariei, J. Santiago-Morales, K. Boltes, P. Letón, I. Iriepa, I. Moraleda, A.R. Fernández-Alba, R. Rosal, Dendrimer-functionalized electrospun nanofibres as dual-action water treatment membranes, Sci. Total Environ. 601–602 (2017) 732–740, https://doi.org/10.1016/j.scitotenv.2017.05.243.

[27] J. Kurczewska, M. Cegłowski, G. Schroeder, Alginate/PAMAM dendrimer – Halloysite beads for removal of cationic and anionic dyes, Int. J. Biol. Macromol. 123 (2019) 398–408, https://doi.org/10.1016/j.ijbiomac.2018.11.119.

[28] D. Guo, N. Muhammad, C. Lou, D. Shou, Y. Zhu, Synthesis of dendrimer functionalized adsorbents for rapid removal of glyphosate from aqueous solution, New J. Chem. 43 (2019) 121–129, https://doi.org/10.1039/C8NJ04433C.

[29] W. Qin, G. Qian, H. Tao, J. Wang, J. Sun, X. Cui, Y. Zhang, X. Zhang, Adsorption of Hg(II) ions by PAMAM dendrimers modified attapulgite composites, React. Funct. Polym. 136 (2019) 75–85, https://doi.org/10.1016/j.reactfunctpolym.2019.01.005.

[30] V. Vatanpour, A. Sanadgol, Surface modification of reverse osmosis membranes by grafting of polyamidoamine dendrimer containing graphene oxide nanosheets for desalination improvement, Desalination 491 (2020), https://doi.org/10.1016/j.desal.2020.114442 114442.

[31] M. Sajid, M.K. Nazal, Ihsanullah, N. Baig, A.M. Osman, Removal of heavy metals and organic pollutants from water using dendritic polymers based adsorbents: A critical review, Separat. Purificat. Technol. 191 (2018) 400–423, https://doi.org/10.1016/j.seppur.2017.09.011.

[32] Y.-L. Han, S.-Y. Kim, T. Kim, K.-H. Kim, J.-W. Park, The role of terminal groups in dendrimer systems for the treatment of organic contaminants in aqueous environments, J. Cleaner Prod. 250 (2020), https://doi.org/10.1016/j.jclepro.2019.119494 119494.

[33] Y. Duan, Y. Song, L. Zhou, Facile synthesis of polyamidoamine dendrimer gel with multiple amine groups as a super adsorbent for highly efficient and selective removal of anionic dyes, J. Colloid Interface Sci. 546 (2019) 351–360, https://doi.org/10.1016/j.jcis.2019.03.073.

[34] K. Lakshmi, R. Rangasamy, Synthetic modification of silica coated magnetite cored PAMAM dendrimer to enrich branched Amine groups and peripheral carboxyl groups for environmental remediation, J. Mol. Struct. 1224 (2021), https://doi.org/10.1016/j.molstruc.2020.129081 129081.

[35] H. Akbari, M. Gholami, H. Akbari, A. Adibzadeh, L. Taghavi, B. Hayati, S. Nazari, Poly (amidoamine) generation 6 functionalized Fe3O4@SiO2/GPTMS core–shell magnetic NPs as a new adsorbent for Arsenite adsorption: kinetic, isotherm and thermodynamic studies, J Environ Health Sci Engineer. 18 (2020) 253–265, https://doi.org/10.1007/s40201-020-00461-4.

[36] Z. Liu, X. Lin, X. Liu, J. Li, W. Zhou, H. Gao, S. Zhang, R. Lu, Magnetic nanoparticles modified with hyperbranched polyamidoamine for the extraction of benzoylurea insecticides prior to their quantitation by HPLC, Microchim. Acta 186 (2019) 351, https://doi.org/10.1007/s00604-019-3450-5.

[37] J. Kurczewska, M. Cegłowski, G. Schroeder, PAMAM-halloysite Dunino hybrid as an effective adsorbent of ibuprofen and naproxen from aqueous solutions, Appl. Clay Sci. 190 (2020), https://doi.org/10.1016/j.clay.2020.105603 105603.

[38] D. Yuan, L. Chen, X. Xiong, Q. Zhang, S. Liao, L. Yuan, Y. Wang, Synthesis of PAMAM dendron functionalized superparamagnetic polymer microspheres for highly efficient sorption of uranium(VI), J. Radioanal. Nucl. Chem. 309 (2016) 1227–1240, https://doi.org/10.1007/s10967-016-4735-3.

[39] H. Viltres, O.F. Odio, Mark. C. Biesinger, G. Montiel, R. Borja, E. Reguera, Preparation of Amine- and Disulfide-Containing PAMAM-Based Dendrons for the Functionalization of Hydroxylated Surfaces: XPS as Structural Sensor, ChemistrySelect. 5 (2020) 4875–4884, https://doi.org/10.1002/slct.202000432.

[40] K. Tokarczyk, B. Jachimska, Characterization of G4 PAMAM dendrimer complexes with 5-fluorouracil and their interactions with bovine serum albumin, Colloids Surf. A 561 (2019) 357–363, https://doi.org/10.1016/j.colsurfa.2018.10.080.

[41] P. Ilaiyaraja, A.K.S. Deb, D. Ponraju, Removal of uranium and thorium from aqueous solution by ultrafiltration (UF) and PAMAM dendrimer assisted ultrafiltration (DAUF), J. Radioanal. Nucl. Chem. 303 (2015) 441–450, https://doi.org/10.1007/s10967-014-3462-x.

[42] M. Kostić, M. Đorđević, J. Mitrović, N. Velinov, D. Bojić, M. Antonijević, A. Bojić, Removal of cationic pollutants from water by xanthated corn cob: optimization, kinetics, thermodynamics, and prediction of purification process, Environ. Sci. Pollut. Res. 24 (2017) 17790–17804, https://doi.org/10.1007/s11356-017-9419-1.

[43] S. Wadhawan, A. Jain, J. Nayyar, S.K. Mehta, Role of nanomaterials as adsorbents in heavy metal ion removal from waste water: A review, J. Water Process Eng. 33 (2020), https://doi.org/10.1016/j.jwpe.2019.101038 101038.

[44] M.T. Yagub, T.K. Sen, S. Afroze, H.M. Ang, Dye and its removal from aqueous solution by adsorption: A review, Adv. Colloid Interface Sci. 209 (2014) 172–184, https://doi.org/10.1016/j.cis.2014.04.002.

[45] L. Liu, B. Zhang, Y. Zhang, Y. He, L. Huang, S. Tan, X. Cai, Simultaneous Removal of Cationic and Anionic Dyes from Environmental Water Using Montmorillonite-Pillared Graphene Oxide, J. Chem. Eng. Data 60 (2015) 1270–1278, https://doi.org/10.1021/je5009312.

[46] A. Maleki, B. Hayati, F. Najafi, F. Gharibi, S.W. Joo, Heavy metal adsorption from industrial wastewater by PAMAM/TiO2 nanohybrid: Preparation, characterization and adsorption studies, J. Mol. Liq. 224 (2016) 95–104, https://doi.org/10.1016/j.molliq.2016.09.060.

[47] R. Ebrahimi, B. Hayati, B. Shahmoradi, R. Rezaee, M. Safari, A. Maleki, K. Yetilmezsoy, Adsorptive removal of nickel and lead ions from aqueous solutions by poly (amidoamine) (PAMAM) dendrimers (G 4), Environ. Technol. Innovation 12 (2018) 261–272, https://doi.org/10.1016/j.eti.2018.10.001.

[48] Z. Zarghami, A. Akbari, A.M. Latifi, M.A. Amani, Design of a new integrated chitosan-PAMAM dendrimer biosorbent for heavy metals removing and study of its adsorption kinetics and thermodynamics, Bioresour. Technol. 205 (2016) 230–238, https://doi.org/10.1016/j.biortech.2016.01.052.

[49] Y. Wang, Q. Lu, Dendrimer functionalized nanocrystalline cellulose for Cu(II) removal, Cellulose 27 (2020) 2173–2187, https://doi.org/10.1007/s10570-019-02919-7.

[50] B. Ren, K. Wang, B. Zhang, H. Li, Y. Niu, H. Chen, Z. Yang, X. Li, H. Zhang, Adsorption behavior of PAMAM dendrimers functionalized silica for Cd(II) from aqueous solution: Experimental and theoretical calculation, J. Taiwan Inst. Chem. Eng. 101 (2019) 80–91, https://doi.org/10.1016/j.jtice.2019.04.037.

[51] R. Yin, Y. Niu, B. Zhang, H. Chen, Z. Yang, L. Yang, Y. Cu, Removal of Cr(III) from aqueous solution by silica-gel/PAMAM dendrimer hybrid materials, Environ. Sci. Pollut. Res. 26 (2019) 18098–18112, https://doi.org/10.1007/s11356-019-05220-z.

[52] W. Qiao, P. Zhang, L. Sun, S. Ma, W. Xu, S. Xu, Y. Niu, Adsorption performance and mechanism of Schiff base functionalized polyamidoamine dendrimer/silica for aqueous Mn(II) and Co(II), Chin. Chem. Lett. 31 (2020) 2742–2746, https://doi.org/10.1016/j.cclet.2020.04.036.

[53] S. Ghodsi, M. Behbahani, M. Yegane Badi, M. Ghambarian, H.R. Sobhi, A. Esrafili, A new dendrimer-functionalized magnetic nanosorbent for the efficient adsorption and subsequent trace measurement of Hg (II) ions in wastewater samples, J. Mol. Liq. 323 (2021), https://doi.org/10.1016/j.molliq.2020.114472 114472.

[54] N.K. Gupta, A. Gupta, 2D and 3D carbon-based adsorbents for an efficient removal of HgII ions: A review, FlatChem. 11 (2018) 1–14, https://doi.org/10.1016/j.flatc.2018.11.002.

[55] F. Einollahi Peer, N. Bahramifar, H. Younesi, Removal of Cd (II), Pb (II) and Cu (II) ions from aqueous solution by polyamidoamine dendrimer grafted magnetic graphene oxide nanosheets, J. Taiwan Inst. Chem. Eng. 87 (2018) 225–240, https://doi.org/10.1016/j.jtice.2018.03.039.

[56] B. Hayati, A. Maleki, F. Najafi, H. Daraei, F. Gharibi, G. McKay, Super high removal capacities of heavy metals (Pb 2+ and Cu 2+) using CNT dendrimer, J. Hazard. Mater. 336 (2017) 146–157, https://doi.org/10.1016/j.jhazmat.2017.02.059.

[57] M. Neaz Morshed, N. Behary, N. Bouazizi, J. Vieillard, J. Guan, J. Le Derf, V. Nierstrasz, Modification of fibrous membrane for organic and pathogenic contaminants removal: from design to application, RSC Adv. 10 (2020) 13155–13173, https://doi.org/10.1039/D0RA01362E.

[58] H. Sun, X. Zhang, Y. He, D. Zhang, X. Feng, Y. Zhao, L. Chen, Preparation of PVDF-g-PAA-PAMAM membrane for efficient removal of copper ions, Chem. Eng. Sci. 209 (2019), https://doi.org/10.1016/j.ces.2019.115186 115186.

[59] H.-R. Kim, J.-W. Jang, J.-W. Park, Carboxymethyl chitosan-modified magnetic-cored dendrimer as an amphoteric adsorbent, J. Hazard. Mater. 317 (2016) 608–616, https://doi.org/10.1016/j.jhazmat.2016.06.025.

[60] P.F. Lito, J.P.S. Aniceto, C.M. Silva, Removal of Anionic Pollutants from Waters and Wastewaters and Materials Perspective for Their Selective Sorption, Water Air Soil Pollut. 223 (2012) 6133–6155, https://doi.org/10.1007/s11270-012-1346-7.

[61] S. Pulkka, M. Martikainen, A. Bhatnagar, M. Sillanpää, Electrochemical methods for the removal of anionic contaminants from water – A review, Sep. Purif. Technol. 132 (2014) 252–271, https://doi.org/10.1016/j.seppur.2014.05.021.

[62] X. Xu, B. Gao, B. Jin, Q. Yue, Removal of anionic pollutants from liquids by biomass materials: A review, J. Mol. Liq. 215 (2016) 565–595, https://doi.org/10.1016/j.molliq.2015.12.101.

[63] Y. Xie, J. Lin, H. Lin, Y. Jiang, J. Liang, H. Wang, S. Tu, J. Li, Removal of anionic hexavalent chromium and methyl orange pollutants by using imidazolium-based mesoporous poly(ionic liquid) as efficient adsorbents in column, J. Hazard. Mater. 392 (2020), https://doi.org/10.1016/j.jhazmat.2020.122496 122496.

[64] A. Alighardashi, Z. Kashitarash Esfahani, F. Najafi, A. Afkhami, N. Hassani, Development and Application of Graphene Oxide/Poly-Amidoamines Dendrimers (GO/PAMAMs) Nano-Composite for Nitrate Removal from Aqueous Solutions, Environ. Process. 5 (2018) 41–64, https://doi.org/10.1007/s40710-017-0279-y.

[65] S.A. Hassan, A.S. Darwish, H.M. Gobara, N.E.A. Abed-elsatar, S.R. Fouda, Interaction profiles in poly (amidoamine) dendrimer/montmorillonite or rice straw ash hybrids-immobilized magnetite nanoparticles governing their removal efficiencies of various pollutants in wastewater, J. Mol. Liq. 230 (2017) 353–369, https://doi.org/10.1016/j.molliq.2017.01.060.

[66] M. Mirzaie, A. Rashidi, H.-A. Tayebi, M.E. Yazdanshenas, Removal of Anionic Dye from Aqueous Media by Adsorption onto SBA-15/Polyamidoamine Dendrimer Hybrid: Adsorption Equilibrium and Kinetics, J. Chem. Eng. Data 62 (2017) 1365–1376, https://doi.org/10.1021/acs.jced.6b00917.

[67] G. Chizari Fard, M. Mirjalili, A. Almasian, F. Najafi, PAMAM grafted α-Fe 2 O 3 nanofiber: Preparation and dye removal ability from binary system, J. Taiwan Inst. Chem. Eng. 80 (2017) 156–167, https://doi.org/10.1016/j.jtice.2017.04.018.

[68] M. Rafi, B. Samiey, C.-H. Cheng, Study of Adsorption Mechanism of Congo Red on Graphene Oxide/PAMAM Nanocomposite, Materials. 11 (2018) 496, https://doi.org/10.3390/ma11040496.

[69] M.H. Kanani-Jazi, S. Akbari, M.A. Haghighat Kish, Efficient removal of Cr (VI) from aqueous solution by halloysite/poly(amidoamine) dendritic nano-hybrid materials: kinetic, isotherm and thermodynamic studies, Adv. Powder Technol. 31 (2020) 4018–4030, https://doi.org/10.1016/j.apt.2020.08.004.

[70] S.M. Prabhu, R.R. Pawar, K. Sasaki, C.M. Park, A mechanistic investigation of highly stable nano ZrO2 decorated nitrogen-rich azacytosine tethered graphene oxide-based dendrimer for the removal of arsenite from water, Chem. Eng. J. 370 (2019) 1474–1484, https://doi.org/10.1016/j.cej.2019.03.277.

[71] D. Fatta-Kassinos, S. Meric, A. Nikolaou, Pharmaceutical residues in environmental waters and wastewater: current state of knowledge and future research, Anal. Bioanal. Chem. 399 (2011) 251–275, https://doi.org/10.1007/s00216-010-4300-9.

[72] B.F. da Silva, A. Jelic, R. López-Serna, A.A. Mozeto, M. Petrovic, D. Barceló, Occurrence and distribution of pharmaceuticals in surface water, suspended solids and sediments of the Ebro river basin, Spain, Chemosphere. 85 (2011) 1331–1339, https://doi.org/10.1016/j.chemosphere.2011.07.051.

[73] I. Sirés, E. Brillas, Remediation of water pollution caused by pharmaceutical residues based on electrochemical separation and degradation technologies: A review, Environ. Int. 40 (2012) 212–229, https://doi.org/10.1016/j.envint.2011.07.012.

[74] V. Cao, A. Yunessnia Lehi, M. Bojaran, M. Fattahi, Treatment of Lasalocid A, Salinomycin and Semduramicin as ionophore antibiotics in pharmaceutical wastewater by PAMAM-coated membranes, Environ. Technol. Innovat. 20 (2020) 101103, https://doi.org/10.1016/j.eti.2020.101103.

[75] J.T. Khutlane, K.R. Koch, R. Malgas-Enus, Competitive removal of PGMs from aqueous solutions via dendrimer modified magnetic nanoparticles, SN Appl. Sci. 2 (2020) 1125, https://doi.org/10.1007/s42452-020-2922-x.

[76] V.T. Nguyen, S. Riaño, K. Binnemans, Separation of precious metals by split-anion extraction using water-saturated ionic liquids, Green Chem. 22 (2020) 8375–8388, https://doi.org/10.1039/D0GC02356F.

[77] W. Zhao, Z. Chen, X. Yang, X. Qian, C. Liu, D. Zhou, T. Sun, M. Zhang, G. Wei, P. D. Dissanayake, Y.S. Ok, Recent advances in photocatalytic hydrogen evolution with high-performance catalysts without precious metals, Renew. Sustain. Energy Rev. 132 (2020), https://doi.org/10.1016/j.rser.2020.110040 110040.

[78] S.K. Padamata, A.S. Yasinskiy, P.V. Polyakov, E.A. Pavlov, D.Yu. Varyukhin, Recovery of Noble Metals from Spent Catalysts: A Review, Metall. Mater. Trans. B 51 (2020) 2413–2435, https://doi.org/10.1007/s11663-020-01913-w.

[79] C.-H. Yen, H.-L. Lien, J.-S. Chung, H.-D. Yeh, Adsorption of precious metals in water by dendrimer modified magnetic nanoparticles, J. Hazard. Mater. 322 (2017) 215–222, https://doi.org/10.1016/j.jhazmat.2016.02.029.

[80] H. Li, Y. Niu, Z. Xue, Q. Mu, K. Wang, R. Qu, H. Chen, L. Bai, H. Yang, D. Wei, Adsorption property and mechanism of PAMAM dendrimer/silica gel hybrids for Fe(III) and Ag(I) from N,N-dimethylformamide, J. Mol. Liquids 273 (2019) 305–313, https://doi.org/10.1016/j.molliq.2018.10.039.

[81] M.S. Diallo, M.R. Kotte, M. Cho, Mining Critical Metals and Elements from Seawater: Opportunities and Challenges, Environ. Sci. Technol. 49 (2015) 9390–9399, https://doi.org/10.1021/acs.est.5b00463.

[82] L. Luan, B. Tang, Y. Liu, A. Wang, B. Zhang, W. Xu, Y. Niu, Selective capture of Hg(II) and Ag(I) from water by sulfur-functionalized polyamidoamine dendrimer/magnetic Fe3O4 hybrid materials, Sep. Purif. Technol. 257 (2021), https://doi.org/10.1016/j.seppur.2020.117902 117902.

[83] Y. Zhang, R. Qu, C. Sun, C. Ji, H. Chen, P. Yin, Improved synthesis of silica-gel-based dendrimer-like highly branched polymer as the Au(III) adsorbents, Chem. Eng. J. 270 (2015) 110–121, https://doi.org/10.1016/j.cej.2015.02.006.

[84] P. Zhang, Y. Niu, W. Qiao, Z. Xue, L. Bai, H. Chen, Experimental and DFT investigation on the adsorption mechanism of silica gel supported sulfur-capped PAMAM dendrimers for Ag(I), J. Mol. Liq. 263 (2018) 390–398, https://doi.org/10.1016/j.molliq.2018.05.023.

[85] S. Sharma, B. Singh, V.K. Manchanda, Phytoremediation: role of terrestrial plants and aquatic macrophytes in the remediation of radionuclides and heavy metal contaminated soil and water, Environ. Sci. Pollut. Res. 22 (2015) 946–962, https://doi.org/10.1007/s11356-014-3635-8.

[86] W. Gwenzi, L. Mangori, C. Danha, N. Chaukura, N. Dunjana, E. Sanganyado, Sources, behaviour, and environmental and human health risks of high-technology rare earth elements as emerging contaminants, Sci. Total Environ. 636 (2018) 299–313, https://doi.org/10.1016/j.scitotenv.2018.04.235.

[87] N. Das, D. Das, Recovery of rare earth metals through biosorption: An overview, J. Rare Earths 31 (2013) 933–943, https://doi.org/10.1016/S1002-0721(13)60009-5.

[88] K.T. Rim, K.H. Koo, J.S. Park, Toxicological Evaluations of Rare Earths and Their Health Impacts to Workers: A Literature Review, Safety and Health at Work. 4 (2013) 12–26, https://doi.org/10.5491/SHAW.2013.4.1.12.

[89] J. Rogowska, E. Olkowska, W. Ratajczyk, L. Wolska, Gadolinium as a new emerging contaminant of aquatic environments, Environ. Toxicol. Chem. 37 (2018) 1523–1534, https://doi.org/10.1002/etc.4116.

[90] N.K. Gupta, A. Gupta, P. Ramteke, H. Sahoo, A. Sengupta, Biosorption-a green method for the preconcentration of rare earth elements (REEs) from waste solutions: A review, J. Mol. Liq. 274 (2019) 148–164, https://doi.org/10.1016/j.molliq.2018.10.134.

[91] A. Sengupta, N.K. Gupta, MWCNTs based sorbents for nuclear waste management: A review, J. Environ. Chem. Eng. 5 (2017) 5099–5114, https://doi.org/10.1016/j.jece.2017.09.054.

[92] P. Kumar, A. Sengupta, A.K. Singha Deb, K. Dasgupta, Sk.M. Ali, Understanding the sorption behavior of Pu4+ on poly(amidoamine) dendrimer functionalized carbon nanotube: sorption equilibrium, mechanism, kinetics, radiolytic stability, and back-extraction studies, Radiochim. Acta. 105 (2017). https://doi.org/10.1515/ract-2016-2722.

[93] A. Sengupta, A.K.S. Deb, N.K. Gupta, P. Kumar, K. Dasgupta, Sk.M. Ali, Evaluation of 1st and 2nd generation of poly(amidoamine) dendrimer functionalized carbon nanotubes for the efficient removal of neptunium, J. Radioanal. Nucl. Chem. 315 (2018) 331–340. https://doi.org/10.1007/s10967-017-5652-9.

[94] P. Kumar, A. Sengupta, A.K.S. Deb, Sk.M. Ali, Poly(amidoamine) Dendrimer Functionalized Carbon Nanotube for Efficient Sorption of Trivalent f-Elements: A Comparison Between 1st And 2nd Generation, ChemistrySelect. 2 (2017) 975–985. https://doi.org/10.1002/slct.201601550.

[95] A.F. Shaaban, A.A. Khalil, T.A. Lasheen, E.S.A. Nouh, H. Ammar, Polyamidoamine dendrimers modified silica gel for uranium(VI) removal from aqueous solution using batch and fixed–bed column, Dwt. 102 (2008) 197–210, https://doi.org/10.5004/dwt.2018.21813.

[96] N. He, H. Li, C. Cheng, H. Dong, X. Lu, J. Wen, X. Wang, Enhanced marine applicability of adsorbent for uranium via synergy of hyperbranched poly (amido amine) and amidoxime groups, Chem. Eng. J. 395 (2020), https://doi.org/10.1016/j.cej.2020.125162 125162.

[97] N. Priyadarshini, P. Ilaiyaraja, Adsorption of U(VI) and Th(IV) from simulated nuclear waste using PAMAM and DGA functionalized PAMAM dendron grafted styrene divinylbenzene chelating resins, Chem. Pap. 73 (2019) 2879–2884, https://doi.org/10.1007/s11696-019-00830-w.

[98] S. Pahan, S. Panja, D. Banerjee, P.S. Dhami, J.S. Yadav, C.P. Kaushik, Preparation of chitosan functionalized polyamidoamine for the separation of trivalent

lanthanides from acidic waste solution, Radiochim. Acta 107 (2019) 415–422, https://doi.org/10.1515/ract-2018-3022.

[99] Y.-R. Lee, S. Zhang, K. Yu, J. Choi, W.-S. Ahn, Poly(amidoamine) dendrimer immobilized on mesoporous silica foam (MSF) and fibrous nano-silica KCC-1 for Gd3+ adsorption in water, Chem. Eng. J. 378 (2019), https://doi.org/10.1016/j.cej.2019.122133 122133.

[100] A.N. Ebelegi, N. Ayawei, A.K. Inengite, D. Wankasi, Generation-3 Polyamidoamine Dendrimer-Silica Composite: Preparation and Cd(II) Removal Capacity, J. Chem. 2020 (2020) 1–11, https://doi.org/10.1155/2020/6662402.

[101] A. Almasian, M.E. Olya, N.M. Mahmoodi, Synthesis of polyacrylonitrile/polyamidoamine composite nanofibers using electrospinning technique and their dye removal capacity, J. Taiwan Inst. Chem. Eng. 49 (2015) 119–128, https://doi.org/10.1016/j.jtice.2014.11.027.

[102] A. Almasian, M.E. Olya, N.M. Mahmoodi, E. Zarinabadi, Grafting of polyamidoamine dendrimer on polyacrylonitrile nanofiber surface: synthesis and optimization of anionic dye removal process by response surface methodology method, DWT. 147 (2019) 343–361, https://doi.org/10.5004/dwt.2019.23676.

[103] F. Shahamati Fard, S. Akbari, E. Pajootan, M. Arami, Enhanced acidic dye adsorption onto the dendrimer-based modified halloysite nanotubes, Desalin. Water Treat. 57 (2016) 26222–26239, https://doi.org/10.1080/19443994.2016.1160437.

[104] F. Zhang, S. He, C. Zhang, Z. Peng, Adsorption kinetics and thermodynamics of acid Bordeaux B from aqueous solution by graphene oxide/PAMAMs, Water Sci. Technol. 72 (2015) 1217–1225, https://doi.org/10.2166/wst.2015.328.

[105] S. Zhou, A. Xue, Y. Zhang, M. Li, K. Li, Y. Zhao, W. Xing, Novel polyamidoamine dendrimer-functionalized palygorskite adsorbents with high adsorption capacity for Pb2+ and reactive dyes, Appl. Clay Sci. 107 (2015) 220–229, https://doi.org/10.1016/j.clay.2015.01.032.

[106] S. Kusakari, K. Ishidu, Y. Kimura, K. Yamada, Functionalization of Halloysite Nanotubes with Poly(amidoamine) Dendrimers and Their Application to Adsorptive Removal of Hexavalent Chromium, Trans. Mat. Res. Soc. Japan. 44 (2019) 171–176. https://doi.org/10.14723/tmrsj.44.171.

[107] L. Samuel, R. Wang, G. Dubois, R. Allen, R. Wojtecki, Y.-H. La, Amine-functionalized, multi-arm star polymers: A novel platform for removing glyphosate from aqueous media, Chemosphere 169 (2017) 437–442, https://doi.org/10.1016/j.chemosphere.2016.11.049.

[108] Q. Zhou, Y. Wu, Y. Sun, X. Sheng, Y. Tong, J. Guo, B. Zhou, J. Zhao, Magnetic polyamidoamine dendrimers for magnetic separation and sensitive determination of organochlorine pesticides from water samples by high-performance liquid chromatography, J. Environ. Sci. 102 (2021) 64–73, https://doi.org/10.1016/j.jes.2020.09.005.

[109] H. Alinezhad, A. Amiri, M. Tarahomi, B. Maleki, Magnetic solid-phase extraction of non-steroidal anti-inflammatory drugs from environmental water samples using polyamidoamine dendrimer functionalized with magnetite nanoparticles as a sorbent, Talanta 183 (2018) 149–157, https://doi.org/10.1016/j.talanta.2018.02.069.

[110] P. Ilaiyaraja, A.K.S. Deb, D. Ponraju, Sk.M. Ali, B. Venkatraman, Surface Engineering of PAMAM-SDB Chelating Resin with Diglycolamic Acid (DGA) Functional Group for Efficient Sorption of U(VI) and Th(IV) from Aqueous Medium, J. Hazard. Mater. 328 (2017) 1–11, https://doi.org/10.1016/j.jhazmat.2017.01.001.

[111] C. Zhang, F. Zhang, L. Li, K. Zhang, Adsorption Rare Earth Metal Ions from Aqueous Solution by Polyamidoamine Dendrimer Functionalized Soy Hull, Waste Biomass Valor. 7 (2016) 1211–1219, https://doi.org/10.1007/s12649-016-9514-4.

[112] B. Ekwurzel, J. Boneham, M.W. Dalton, R. Heede, R.J. Mera, M.R. Allen, P.C. Frumhoff, The rise in global atmospheric CO2, surface temperature, and sea level from emissions traced to major carbon producers, Clim. Change 144 (2017) 579–590, https://doi.org/10.1007/s10584-017-1978-0.

[113] D.Y.C. Leung, G. Caramanna, M.M. Maroto-Valer, An overview of current status of carbon dioxide capture and storage technologies, Renew. Sustain. Energy Rev. 39 (2014) 426–443, https://doi.org/10.1016/j.rser.2014.07.093.

[114] A. Samanta, A. Zhao, G.K.H. Shimizu, P. Sarkar, R. Gupta, Post-Combustion CO₂ Capture Using Solid Sorbents: A Review, Ind. Eng. Chem. Res. 51 (2012) 1438–1463, https://doi.org/10.1021/ie200686q.

[115] A.S. Kovvali, K.K. Sirkar, Dendrimer Liquid Membranes: CO₂ Separation from Gas Mixtures, Ind. Eng. Chem. Res. 40 (2001) 2502–2511, https://doi.org/10.1021/ie0010520.

[116] J. Chau, G. Obuskovic, X. Jie, T. Mulukutla, K.K. Sirkar, Solubilities of CO₂ and Helium in an Ionic Liquid Containing Poly(amidoamine) Dendrimer Gen 0, Ind. Eng. Chem. Res. 52 (2013) 10484–10494, https://doi.org/10.1021/ie303426q.

[117] T. Mulukutla, J. Chau, D. Singh, G. Obuskovic, K.K. Sirkar, Novel membrane contactor for CO₂ removal from flue gas by temperature swing absorption, J. Membr. Sci. 493 (2015) 321–328, https://doi.org/10.1016/j.memsci.2015.06.039.

[118] S. Duan, T. Kai, T. Saito, K. Yamazaki, K. Ikeda, Effect of Cross-Linking on the Mechanical and Thermal Properties of Poly(amidoamine) Dendrimer/Poly(vinyl alcohol) Hybrid Membranes for CO2 Separation, Membranes. 4 (2014) 200–209, https://doi.org/10.3390/membranes4020200.

[119] S. Duan, T. Kouketsu, S. Kazama, K. Yamada, Development of PAMAM dendrimer composite membranes for CO2 separation, J. Membr. Sci. 283 (2006) 2–6, https://doi.org/10.1016/j.memsci.2006.06.026.

[120] R. Borgohain, B. Mandal, Thermally stable and moisture responsive carboxymethyl chitosan/dendrimer/hydrotalcite membrane for CO2 separation, J. Membr. Sci. 608 (2020), https://doi.org/10.1016/j.memsci.2020.118214 118214.

[121] J. Chau, X. Jie, K.K. Sirkar, Polyamidoamine-facilitated poly(ethylene glycol)/ionic liquid based pressure swing membrane absorption process for CO2 removal from shifted syngas, Chem. Eng. J. 305 (2016) 212–220, https://doi.org/10.1016/j.cej.2015.09.120.

[122] K.J. Shah, T. Imae, A. Shukla, Selective capture of CO₂ by poly(amido amine) dendrimer-loaded organoclays, RSC Adv. 5 (2015) 35985–35992, https://doi.org/10.1039/C5RA04904K.

[123] M. Miyamoto, A. Takayama, S. Uemiya, K. Yogo, Study of Gas Adsorption Properties of Amidoamine-Loaded Mesoporous Silica for Examing Its Use in CO2 Separation, J. Chem. Eng. Japan / JCEJ. 45 (2012) 395–400, https://doi.org/10.1252/jcej.12we006.

[124] Md.B. Haider, Z. Hussain, R. Kumar, CO2 absorption and kinetic study in ionic liquid amine blends, J. Mol. Liq. 224 (2016) 1025–1031, https://doi.org/10.1016/j.molliq.2016.10.044.

[125] T. Mulukutla, G. Obuskovic, K.K. Sirkar, Novel scrubbing system for post-combustion CO2 capture and recovery: Experimental studies, J. Membr. Sci. 471 (2014) 16–26, https://doi.org/10.1016/j.memsci.2014.07.037.

[126] V.B. Cashin, D.S. Eldridge, A. Yu, D. Zhao, Surface functionalization and manipulation of mesoporous silica adsorbents for improved removal of pollutants: a review, Environ. Sci. Water Res. Technol. 4 (2018) 110–128, https://doi.org/10.1039/C7EW00322F.

[127] H.-J. Kim, H.-C. Yang, D.-Y. Chung, I.-H. Yang, Y.J. Choi, J. Moon, Functionalized Mesoporous Silica Membranes for CO₂ Separation Applications, J. Chem. 2015 (2015) 1–9, https://doi.org/10.1155/2015/202867.

[128] T.-L. Chew, A.L. Ahmad, S. Bhatia, Ordered mesoporous silica (OMS) as an adsorbent and membrane for separation of carbon dioxide (CO2), Adv. Colloid Interface Sci. 153 (2010) 43–57, https://doi.org/10.1016/j.cis.2009.12.001.

[129] S. Zhang, C. Chen, W.-S. Ahn, Recent progress on CO2 capture using amine-functionalized silica, Curr. Opin. Green Sustainable Chem. 16 (2019) 26–32, https://doi.org/10.1016/j.cogsc.2018.11.011.

[130] B. Fadhel, M. Hearn, A. Chaffee, CO2 adsorption by PAMAM dendrimers: Significant effect of impregnation into SBA-15, Micropor. Mesopor. Mater. 123 (2009) 140–149, https://doi.org/10.1016/j.micromeso.2009.03.040.

[131] G. Gómez-Pozuelo, E.S. Sanz-Pérez, A. Arencibia, P. Pizarro, R. Sanz, D.P. Serrano, CO2 adsorption on amine-functionalized clays, Micropor. Mesopor. Mater. 282 (2019) 38–47, https://doi.org/10.1016/j.micromeso.2019.03.012.

[132] N. Chouikhi, J.A. Cecilia, E. Vilarrasa-García, S. Besghaier, M. Chlendi, F.I. Franco Duro, E. Rodriguez Castellon, M. Bagane, CO2 Adsorption of Materials Synthesized from Clay Minerals: A Review, Minerals 9 (2019) 514, https://doi.org/10.3390/min9090514.

[133] K.J. Shah, T. Imae, M. Ujihara, S.-J. Huang, P.-H. Wu, S.-B. Liu, Poly(amido amine) dendrimer-incorporated organoclays as efficient adsorbents for capture of NH3 and CO2, Chem. Eng. J. 312 (2017) 118–125, https://doi.org/10.1016/j.cej.2016.11.125.

[134] S. Duan, I. Taniguchi, T. Kai, S. Kazama, Poly(amidoamine) dendrimer/poly(vinyl alcohol) hybrid membranes for CO2 capture, J. Membr. Sci. 423–424 (2012) 107–112, https://doi.org/10.1016/j.memsci.2012.07.037.

[135] S. Duan, T. Kai, I. Taniguchi, S. Kazama, Development of poly(amidoamine) dendrimer/poly(vinyl alcohol) hybrid membranes for CO₂ separation, Desalin. Water Treat. 51 (2013) 5337–5342, https://doi.org/10.1080/19443994.2013.768797.

[136] Shuhong. Duan, Ikuo. Taniguchi, Teruhiko. Kai, Shingo. Kazama, Development of poly(amidoamine) dendrimer/polyvinyl alcohol hybrid membranes for CO2 capture at elevated pressures, Energy Proc. 37 (2013) 924–931. https://doi.org/10.1016/j.egypro.2013.05.187.

[137] S. Duan, T. Kai, I. Taniguchi, S. Kazama, Development of Poly(Amidoamine) Dendrimer/ Poly(Ethylene Glycol) Hybrid Membranes for CO2 Capture at Elevated Pressures, Energy Procedia 63 (2014) 167–173, https://doi.org/10.1016/j.egypro.2014.11.017.

[138] I. Taniguchi, S. Duan, S. Kazama, Y. Fujioka, Facile fabrication of a novel high performance CO2 separation membrane: Immobilization of poly(amidoamine) dendrimers in poly(ethylene glycol) networks, J. Membr. Sci. 322 (2008) 277–280, https://doi.org/10.1016/j.memsci.2008.05.067.

[139] J.H. Lee, J.Y. Lim, M.S. Park, J.H. Kim, Improvement in the CO₂ Permeation Properties of High-Molecular-Weight Poly(ethylene oxide): Use of Amine-Branched Poly(amidoamine) Dendrimer, Macromolecules 51 (2018) 8800–8807, https://doi.org/10.1021/acs.macromol.8b02037.

[140] I. Taniguchi, S. Duan, T. Kai, S. Kazama, H. Jinnai, Effect of the phase-separated structure on CO2 separation performance of the poly(amidoamine) dendrimer immobilized in a poly(ethylene glycol) network, J. Mater. Chem. A 1 (2013) 14514, https://doi.org/10.1039/c3ta13711b.

[141] J. Satija, S.K. Chauhan, N. Punjabi, S. Mukherji, Dendrimer Sensors, in: Comprehensive Supramolecular Chemistry II, Elsevier, 2017: pp. 237–259. https://doi.org/10.1016/B978-0-12-409547-2.12632-0.

[142] M. Algarra, B.B. Campos, M.S. Miranda, J.C.G.E. da Silva, CdSe quantum dots capped PAMAM dendrimer nanocomposites for sensing nitroaromatic compounds, Talanta 83 (2011) 1335–1340, https://doi.org/10.1016/j.talanta.2010.10.056.

[143] M. Lin, Y. Liu, C. Liu, Z. Yang, Y. Huang, Sensitive immunosensor for benzo[a]pyrene detection based on dual amplification strategy of PAMAM dendrimer and amino-modified methylene blue/SiO2 core–shell nanoparticles, Biosens.

Bioelectron. 26 (2011) 3761–3767, https://doi.org/10.1016/j.bios.2011.02.028.

[144] Y. Qu, Q. Sun, F. Xiao, G. Shi, L. Jin, Layer-by-Layer self-assembled acetylcholinesterase/PAMAM-Au on CNTs modified electrode for sensing pesticides, Bioelectrochemistry 77 (2010) 139–144, https://doi.org/10.1016/j.bioelechem.2009.08.001.

[145] H. Yin, L. Cui, Q. Chen, W. Shi, S. Ai, L. Zhu, L. Lu, Amperometric determination of bisphenol A in milk using PAMAM–Fe3O4 modified glassy carbon electrode, Food Chem. 125 (2011) 1097–1103, https://doi.org/10.1016/j.foodchem.2010.09.098.

[146] H. Yin, Y. Zhou, S. Ai, Q. Chen, X. Zhu, X. Liu, L. Zhu, Sensitivity and selectivity determination of BPA in real water samples using PAMAM dendrimer and CoTe quantum dots modified glassy carbon electrode, J. Hazard. Mater. 174 (2010) 236–243, https://doi.org/10.1016/j.jhazmat.2009.09.041.

[147] Y. Wu, C. Chen, Q. Zhou, Q.X. Li, Y. Yuan, Y. Tong, H. Wang, X. Zhou, Y. Sun, X. Sheng, Polyamidoamine dendrimer decorated nanoparticles as an adsorbent for magnetic solid-phase extraction of tetrabromobisphenol A and 4-nonylphenol from environmental water samples, J. Colloid Interface Sci. 539 (2019) 361–369, https://doi.org/10.1016/j.jcis.2018.12.064.

[148] Y. Wu, Q. Zhou, Y. Yuan, H. Wang, Y. Tong, Y. Zhan, X. Sheng, Y. Sun, X. Zhou, Enrichment and sensitive determination of phthalate esters in environmental water samples: A novel approach of MSPE-HPLC based on PAMAM dendrimers-functionalized magnetic-nanoparticles, Talanta 206 (2020), https://doi.org/10.1016/j.talanta.2019.120213 120213.

[149] Y. Tong, Q. Zhou, Y. Sun, X. Sheng, B. Zhou, J. Zhao, J. Guo, Magnetic polyamidoamine dendrimer grafted with 4-mercaptobenzoic acid as an adsorbent for preconcentration and sensitive determination of polycyclic aromatic hydrocarbons from environmental water samples, Talanta 224 (2021), https://doi.org/10.1016/j.talanta.2020.121884 121884.

[150] Y. Yuan, Y. Wu, H. Wang, Y. Tong, X. Sheng, Y. Sun, X. Zhou, Q. Zhou, Simultaneous enrichment and determination of cadmium and mercury ions using magnetic PAMAM dendrimers as the adsorbents for magnetic solid phase extraction coupled with high performance liquid chromatography, J. Hazard. Mater. 386 (2020), https://doi.org/10.1016/j.jhazmat.2019.121658 121658.

[151] M.U. Gürbüz, G. Elmacı, A.S. Ertürk, Tren-Cored PAMAM Dendrimer/Silver Nanocomposites: Efficient Colorimetric Sensors for the Determination of Mercury Ions from Aqueous Solutions, ChemistrySelect. 4 (2019) 7715–7721, https://doi.org/10.1002/slct.201901538.

[152] F. Ma, Y. Zhang, H. Qi, Q. Gao, C. Zhang, W. Miao, Ultrasensitive electrogenerated chemiluminescence biosensor for the determination of mercury ion incorporating G4 PAMAM dendrimer and Hg(II)-specific oligonucleotide, Biosens. Bioelectron. 32 (2012) 37–42, https://doi.org/10.1016/j.bios.2011.11.011.

[153] B. Babamiri, A. Salimi, R. Hallaj, Switchable electrochemiluminescence aptasensor coupled with resonance energy transfer for selective attomolar detection of Hg2+ via CdTe@CdS/dendrimer probe and Au nanoparticle quencher, Biosens. Bioelectron. 102 (2018) 328–335, https://doi.org/10.1016/j.bios.2017.11.034.

[154] S. Yordanova, I. Grabchev, S. Stoyanov, I. Petkov, New detectors for metal cations and protons based on PAMAM dendrimers modified with 1,8-naphthalimide units, J. Photochem. Photobiol., A 283 (2014) 1–7, https://doi.org/10.1016/j.jphotochem.2014.03.002.

[155] I. Grabchev, D. Staneva, R. Betcheva, Fluorescent Dendrimers As Sensors for Biologically Important Metal Cations, CMC. 19 (2012) 4976–4983, https://doi.org/10.2174/0929867311209024976.

[156] D. Staneva, P. Bosch, A.M. Asiri, L.A. Taib, I. Grabchev, Studying pH dependence of the photophysical properties of a blue emitting fluorescent PAMAM dendrimer and evaluation of its sensor potential, Dyes Pigm. 105 (2014) 114–120, https://doi.org/10.1016/j.dyepig.2014.01.018.

[157] M. Dodangeh, K. Gharanjig, M. Arami, A novel Ag + cation sensor based on polyamidoamine dendrimer modified with 1,8-naphthalimide derivatives, Spectrochim. Acta Part A Mol. Biomol. Spectrosc. 154 (2016) 207–214, https://doi.org/10.1016/j.saa.2015.09.031.

[158] M. Dodangeh, D. Staneva, I. Grabchev, R.-C. Tang, K. Gharanjig, Synthesis, spectral characteristics and sensor ability of new polyamidoamine dendrimers, modified with curcumin, Spectrochim. Acta Part A Mol. Biomol. Spectrosc. 228 (2020), https://doi.org/10.1016/j.saa.2019.117554 117554.

[159] B.B. Campos, M.M. Oliva, R. Contreras-Cáceres, E. Rodriguez-Castellón, J. Jiménez-Jiménez, J.C.G.E. da Silva, M. Algarra, Carbon dots on based folic acid coated with PAMAM dendrimer as platform for Pt(IV) detection, J. Colloid Interface Sci. 465 (2016) 165–173, https://doi.org/10.1016/j.jcis.2015.11.059.

[160] M.P. Militello, R.E. Hernández Ramírez, I.V. Lijanova, C.M. Previtali, S.G. Bertolotti, E.M. Arbeloa, PAMAM dendrimers with a porphyrin core as highly selective binders of Li + in an alkaline mixture. A spectroscopic study, New J. Chem. 43 (2019) 16246–16254, https://doi.org/10.1039/C9NJ04088A.

[161] M.M. Falinski, D.L. Plata, S.S. Chopra, T.L. Theis, L.M. Gilbertson, J.B. Zimmerman, A framework for sustainable nanomaterial selection and design based on performance, hazard, and economic considerations, Nature Nanotech. 13 (2018) 708–714, https://doi.org/10.1038/s41565-018-0120-4.

[162] K. Jain, P. Kesharwani, U. Gupta, N.K. Jain, Dendrimer toxicity: Let's meet the challenge, Int. J. Pharm. 394 (2010) 122–142, https://doi.org/10.1016/j.ijpharm.2010.04.027.

[163] B. Nowack, T.D. Bucheli, Occurrence, behavior and effects of nanoparticles in the environment, Environ. Pollut. 150 (2007) 5–22, https://doi.org/10.1016/j.envpol.2007.06.006.

[164] K.L. Aillon, Y. Xie, N. El-Gendy, C.J. Berkland, M.L. Forrest, Effects of nanomaterial physicochemical properties on in vivo toxicity, Adv. Drug Deliv. Rev. 61 (2009) 457–466, https://doi.org/10.1016/j.addr.2009.03.010.

[165] N. Malik, E.G. Evagorou, R. Duncan, Dendrimer-platinate: a novel approach to cancer chemotherapy, Anticancer Drugs 10 (1999) 767–776, https://doi.org/10.1097/00001813-199909000-00010.

[166] T.C. King Heiden, E. Dengler, W.J. Kao, W. Heideman, R.E. Peterson, Developmental toxicity of low generation PAMAM dendrimers in zebrafish, Toxicol. Appl. Pharmacol. 225 (2007) 70–79, https://doi.org/10.1016/j.taap.2007.07.009.

[167] E.N. Gurzov, B. Wang, E.H. Pilkington, P. Chen, A. Kakinen, W.J. Stanley, S.A. Litwak, E.G. Hanssen, T.P. Davis, F. Ding, P.C. Ke, Inhibition of hIAPP Amyloid Aggregation and Pancreatic β-Cell Toxicity by OH-Terminated PAMAM Dendrimer, Small 12 (2016) 1615–1626, https://doi.org/10.1002/smll.201502317.

[168] W. Wang, W. Xiong, Y. Zhu, H. Xu, X. Yang, Protective effect of PEGylation against poly(amidoamine) dendrimer-induced hemolysis of human red blood cells, J. Biomed. Mater. Res. 9999B (2010) NA-NA. https://doi.org/10.1002/jbm.b.31558.

[169] M. Manunta, B.J. Nichols, P. Hong Tan, P. Sagoo, J. Harper, A.J.T. George, Gene delivery by dendrimers operates via different pathways in different cells, but is enhanced by the presence of caveolin, J. Immunol. Methods 314 (2006) 134–146, https://doi.org/10.1016/j.jim.2006.06.007.

[170] S. Gonzalo, I. Rodea-Palomares, F. Leganés, E. García-Calvo, R. Rosal, F. Fernández-Piñas, First evidences of PAMAM dendrimer internalization in microorganisms of environmental relevance: A linkage with toxicity and oxidative stress, Nanotoxicology. 9 (2015) 706–718, https://doi.org/10.3109/17435390.2014.969345.

[171] A.-N. Petit, T. Debenest, P. Eullaffroy, F. Gagné, Effects of a cationic PAMAM dendrimer on photosynthesis and ROS production of *Chlamydomonas reinhardtii*, Nanotoxicology. 6 (2012) 315–326, https://doi.org/10.3109/17435390.2011.579628.

[172] N. Malik, R. Wiwattanapatapee, R. Klopsch, K. Lorenz, H. Frey, J.W. Weener, E.W. Meijer, W. Paulus, R. Duncan, Dendrimers, J. Controlled Release 65 (2000) 133–148. https://doi.org/10.1016/S0168-3659(99)00246-1.

[173] L. Bodewein, F. Schmelter, S. Di Fiore, H. Hollert, R. Fischer, M. Fenske, Differences in toxicity of anionic and cationic PAMAM and PPI dendrimers in zebrafish embryos and cancer cell lines, Toxicol. Appl. Pharmacol. 305 (2016) 83–92, https://doi.org/10.1016/j.taap.2016.06.008.

[174] A.-N. Petit, P. Eullaffroy, T. Debenest, F. Gagné, Toxicity of PAMAM dendrimers to Chlamydomonas reinhardtii, Aquat. Toxicol. 100 (2010) 187–193, https://doi.org/10.1016/j.aquatox.2010.01.019.

[175] P.C. Naha, H.J. Byrne, Generation of intracellular reactive oxygen species and genotoxicity effect to exposure of nanosized polyamidoamine (PAMAM) dendrimers in PLHC-1 cells in vitro, Aquat. Toxicol. 132–133 (2013) 61–72, https://doi.org/10.1016/j.aquatox.2013.01.020.

[176] S.P. Mukherjee, H.J. Byrne, Polyamidoamine dendrimer nanoparticle cytotoxicity, oxidative stress, caspase activation and inflammatory response: experimental observation and numerical simulation, Nanomed.: Nanotechnol. Biol. Med. 9 (2013) 202–211, https://doi.org/10.1016/j.nano.2012.05.002.

[177] J.-H. Lee, K.E. Cha, M.S. Kim, H.W. Hong, D.J. Chung, G. Ryu, H. Myung, Nanosized polyamidoamine (PAMAM) dendrimer-induced apoptosis mediated by mitochondrial dysfunction, Toxicol. Lett. 190 (2009) 202–207, https://doi.org/10.1016/j.toxlet.2009.07.018.

[178] P.C. Naha, M. Davoren, F.M. Lyng, H.J. Byrne, Reactive oxygen species (ROS) induced cytokine production and cytotoxicity of PAMAM dendrimers in J774A.1 cells, Toxicol. Appl. Pharmacol. 246 (2010) 91–99, https://doi.org/10.1016/j.taap.2010.04.014.

[179] I. Durocher, D. Girard, In vivo proinflammatory activity of generations 0–3 (G0–G3) polyamidoamine (PAMAM) nanoparticles, Inflamm. Res. 65 (2016) 745–755, https://doi.org/10.1007/s00011-016-0959-5.

[180] S.P. Mukherjee, M. Davoren, H.J. Byrne, In vitro mammalian cytotoxicological study of PAMAM dendrimers – Towards quantitative structure activity relationships, Toxicol. In Vitro 24 (2010) 169–177, https://doi.org/10.1016/j.tiv.2009.09.014.

[181] K.-J. Kim, J.-W. Park, Stability and reusability of amine-functionalized magnetic-cored dendrimer for heavy metal adsorption, J. Mater. Sci. 52 (2017) 843–857, https://doi.org/10.1007/s10853-016-0380-z.